

## RESPONSES TO REVIEWERS' COMMENTS

Dear ACP Editorial Board,

We are submitting our revised paper entitled “Contrasting ambient fine particles hygroscopicity derived by HTDMA and HR-AMS measurements between summer and winter in urban Beijing. We are grateful to the two reviewers for their insightful and constructive comments and have revised our paper accordingly to account for the reviewers’ recommendations. Below please find our detailed point-by-point responses (in blue) to the reviewers’ comments (in black) to the manuscript. We believe that we have satisfactorily addressed all criticisms from the two reviewers.

Thank you for your attention to this matter.

Sincerely, Fang Zhang on behalf of all authors

### **Anonymous Referee #1**

In this manuscript in discussion for publication in Atmospheric Chemistry and Physics (acp-2019-583), Xinxin Fan and co-authors present a field study comparing aerosol hygroscopicity in summer months relative to the those measured in winter. Measured hygroscopicity was compared to hygroscopicity based on HR-ToF-AMS measurements of composition for Beijing and northern China. The focus on this work was mixing state as a potential cause of the discrepancy between measured and estimated hygroscopicity. Interesting observations are presented and discussed in a mechanistic framework. This work is part of a larger effort to understand the air quality in China, and is important and timely. I have significant concerns, however,

about the novelty of the study and the presentation of the data, which I have outlined below. The data and study design are not novel, and in fact several of the same authors have written a very similar manuscript (published in ACP: <https://www.atmos-chem-phys.net/18/11739/2018/acp-18-11739-2018.pdf>) from the same field campaign.

The preparation of figures as clear and succinct visual aids to the writing is poor, and the authors invoke limited and dated studies on water uptake by mixtures of compounds. These issues could potentially be resolved with appropriate major revisions.

Regarding the novelty of the manuscript, I would urge the authors to share in the introduction the previous findings for the same dataset or the co-located instruments.

It is not clear at present the degree of overlap but it is not the policy of ACP to publish the same data, analysis, and interpretation twice.

The difference between (for example) the CCN and HTDMA needs to be clearly stated in both the method and the interpretation and discussion of underlying physical processes. If the authors do not differentiate effectively between the scientific questions answered by similar instruments, then the study is essentially the same as the published study. This can likely be resolved but will require careful effort.

Re: We appreciate your comments. The reviewer argued that the paper published in ACP and this currently submitted one is very similar manuscript from the same field campaign. This is probably because that some vague descriptions on instruments in the Section 2.1 which may have misled the reviewer. Indeed, the main data used in

the two papers are from different campaigns, the data used in this work are from two field campaigns during November 16-December 10 of 2016 and May 25- June 18 of 2017 in urban Beijing, however, the published ACP paper just used the data from Xingtai campaign which was conducted during 1 May-15 June 2016. These have been clarified in the revised manuscript (See lines 92-98, 383-393). Furthermore, the previous paper published in ACP focused on investigating and characterizing the aerosol hygroscopicity and CCN activity at the suburban site of Xingtai, which is located about 420 km south of urban Beijing. But in the current submitted paper, we compare the size-resolved hygroscopic parameter ( $\kappa_{gf}$ ) of ambient fine particles derived by an HTDMA (Hygroscopic Tandem Differential Mobility Analyzer) to that (denoted as  $\kappa_{chem}$ ) of calculated by an HR-ToF-AMS (High-resolution Time-of-Flight Aerosol Mass Spectrometer) measurements using a simple rule with a uniform internal mixing hypothesis. We mainly focus on contrasting the disparity of  $\kappa_{gf}$  and  $\kappa_{chem}$  between summer and winter in urban Beijing to reveal the impact of atmospheric processes/sources on aerosols hygroscopicity and to evaluate the uncertainty in estimating particles hygroscopicity with the hypothesis. Only in the last section (Section 3.5) of this paper, we include the observations at other sites (not only Xingtai site) just for comparison with that observed in urban Beijing. Such comparison among different sites is to identify the impact of regional emissions/sources and atmospheric processes under different environments on estimating aerosols hygroscopicity with the uniform internal mixing hypothesis. One important findings of this current paper is that, for the first time, we observe clearly that atmospheric photochemical aging of

aerosols induces a coating effect from field measurement. Such effect leads to 10%-20% underestimation of the hygroscopic parameter if using the uniform internal mixing assumption. The coating effect is found more significant for these >100 nm particles observed in remote or clean regions. Our results suggest that it is critical to parameterize such an impact in model simulations to improve the evaluation of the aerosols indirect effect. In addition, in the revised version, we have made a sensitivity test to examine the effect of temporal variations in actual density of BC and organics caused by the particles aging and local sources on calculating  $\kappa_{chem}$  (see lines 319-346).

The figures have been revised carefully according to the comments (see the revised Fig. 1-Fig. 9).

In addition, more previous studies and references on water uptake by mixtures of compounds have been included in the introduction, and some words about the definition of mixing state have been removed in the revised version. The revised introduction is as follows,

“ ...The hygroscopic properties of both the natural and anthropogenic aerosols, in addition to being affected by its chemical composition (Gunthe et al., 2009), are also affected by the particle mixing state and aging (Schill et al., 2015; Peng et al., 2017). For example, a recent laboratory study shown that the coexisting hygroscopic species have a strong influence on the phase state of particles, thus affecting chemical interactions between inorganic and organic compounds as well as the overall hygroscopicity of mixed particles (Peng et al., 2016). The field measurements also demonstrated that the hydrophobic black carbon particles became hygroscopic with atmospheric mixing and aging by organics (i.e. Peng et al., 2017). In a heavily polluted atmosphere, the aerosol sources and sinks are varied, the physical and chemical processes experienced by the aerosols are complex, and the mixing state and its impact on aerosols hygroscopicity is more complicated. The hygroscopicity of mixed particles and mutual impacts between the components are still poorly understood.

Previous studies have shown that the difference between the  $\kappa$  obtained from H-TDMA or CCNc measurements and that calculated based on the volume mixing ratio of chemical components,  $\kappa_{chem}$ . Laboratory results from Cruz and Pandis (2000) indicate that  $\kappa_{gf}$  of internally mixed ammonium sulfate

and organic matter is higher than  $\kappa_{chem}$  calculated for assumed uniform internal mixing. But Peng et al (2016) found that, for sodium chloride and organic aerosols mixed particles, the measured growth factors by H-TDMA were significantly lower than calculations from the mixing rule methods. In some field studies on aged aerosols, the  $\kappa$  was underestimated by the calculation based on uniform internal mixing assumption and thus lead to an underestimation of CCN concentration (Bougiatioti, et al., 2009; Chang, et al., 2007; Kuwata, et al., 2008; Wang, et al., 2010; Ren et al., 2018). However, for primary emissions dominated periods, the  $\kappa$  value from calculations based on bulk chemical composition was much higher than that measured by H-TDMA measurements (Zhang et al., 2017). The various results from previous studies suggest distinct effects of aerosols mixing state on their hygroscopicity. Overall, to what extent do the differences depend on the mixing state and the extent of aging of the particles, and how the different atmospheric processes and what kinds of mixing structure of the particles may result in those disparity between measured and calculated hygroscopic parameter have not been clearly clarified by the previous studies. A comprehensive and systematic investigation on the cause and magnitude of the effect has been lacking.

In the atmosphere, the  $\kappa$ , which is related to the particle mixing state diversity, varies largely across the size range of ambient fine particles (Rose et al., 2010). Previous study only compared the measured  $\kappa$  to that calculated based on bulk chemical composition (Zhang et al., 2017). Using size-resolved, not bulk, chemical composition measurements in different seasons is expected to provide more comprehensive understanding and insights of how the aerosols mixing state influence on their hygroscopicity, motivating our analysis that employs size-resolved chemical composition measured by an HR-ToF-AMS in this study.....”

The difference between (for example) the CCN<sub>c</sub> and HTDMA has been stated in the revised version (see lines 179-189) or as follows,

“...In addition, we also compare the results from the field campaigns with those from other two sites, Xingtai (XT: 37.18 °N, 114.37 °E), and Xinzhou (XZ: 38.24 °N, 112.43 °E), in North China Plain (Fig. 1). At XZ site, we use the hygroscopic parameter (defined as  $\kappa_{CCN_c}$ ) from size-resolved CCN measurements (Zhang et al., 2014, 2016) for comparison. More detailed descriptions of the method to retrieve  $\kappa_{CCN_c}$  can be found in (Petters and Kreidenweis (2007)). Both of the  $\kappa_{gf}$  and  $\kappa_{CCN_c}$  are derived based on  $\kappa$ -Köhler Theory (Petters and Kreidenweis, 2007). But, different from the  $\kappa_{gf}$  measured by the HTDMA system which is operated at RH of 90%, the  $\kappa_{CCN_c}$  is derived by measuring aerosols CCN activity under the condition of supersaturations with relative humidity of >100%. Previous studies from field measurements and laboratory experiments showed that the  $\kappa_{CCN_c}$  is generally slight larger or smaller than  $\kappa_{gf}$ , but they are basically comparable and can well represent an overall aerosols hygroscopicity (e.g. Carrico et al., 2008; Wex et al., 2009; Good et al., 2010; Irwin et al., 2010; Cerully et al., 2011; Wu et al., 2013; Zhang et al., 2017)...”

Comments on figures and interpretation of figures:

The figures do not always serve as appropriate and helpful guides to the writing. The number of figures in both the manuscript and the supplement could be reduced. Not all figures are discussed, and several figures seem to be entirely redundant. The data

in the figures is difficult to interpret due to the overlapping error bars.

Re: As commented by the reviewer, we have considered how to organize the figures very carefully, and removed most of the figures in both the main manuscript and the supplement in the revised version. In addition, the Figures in the main text were replotted due to the overlapping error bars (see the revised Fig. 1-Fig. 9).

Figure 3: It's not clear why this figure does not take the full page width, as it already seems to exceed a 1-column width. It would be helpful to include markers for "morning traffic," "afternoon traffic," or other factors that influence these timeseries. The reader is without a frame of reference. Also, in the caption it would be helpful to see the location for these time series, or whether these are averaged for all sites.

Re: The figure and caption have been revised per the reviewer's comments (see below),

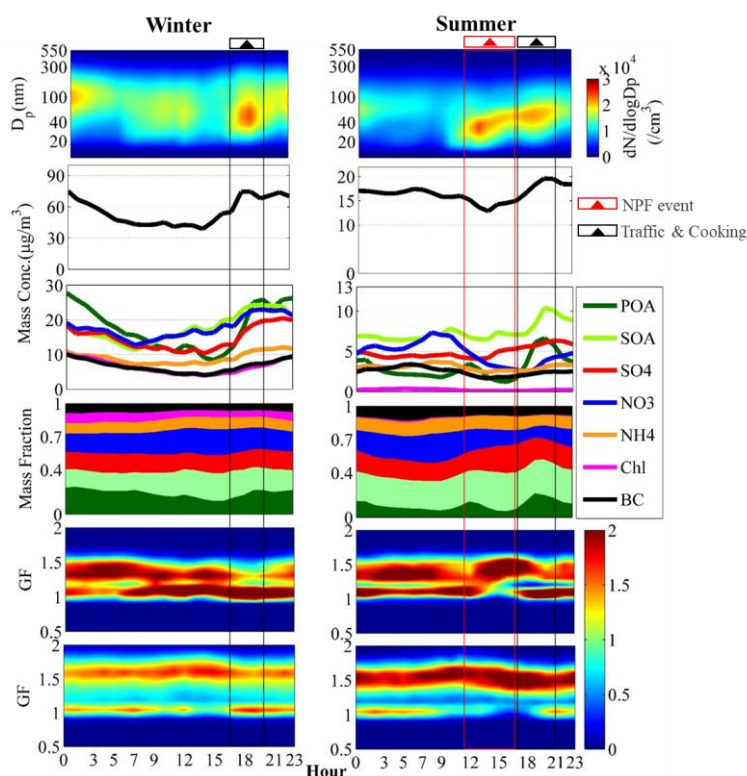


Figure R1. Campaign averaged diurnal variations in particle number size distribution;

mass concentration of PM<sub>1</sub>, bulk mass concentration of main species in PM<sub>1</sub>, mass fraction of chemical composition of PM<sub>1</sub>; and Gf-PDFs for 40 and 150 nm particles in winter (left panels) and summer (right panels) measured in urban Beijing.

Line 218: Figure 3e is referenced before any discussion of all the other panels in Figure 3.

Re: The Fig.3 has been mentioned in the previous paragraph before line 218. However, corresponding revision of the text has been done according to the correction on Fig. 3.

Figure 5: Authors neglect to describe the two lines on each plot; are the R<sup>2</sup> values first or second in the parentheses? Are the 1:1 lines anchored at 0? There seems to be little to no correlation between  $\kappa_{\text{chem}}$  and  $\kappa_{\text{gf}}$ .

Re: Thanks a lot for the careful check. In the revised version, we have added the description about two lines. The first number in parenthesis of each plot is the slope of the fit line, and the second is the correlation coefficient (R<sup>2</sup>). In figure 5, all 1:1 lines are anchored at 0. Exactly, the correlations between  $\kappa_{\text{chem}}$  and  $\kappa_{\text{gf}}$  of the 80, 110, 150, 200 nm particles both in winter and summer are poor due to the large uncertainty in one or both of the calculated parameters. The large uncertainties are likely due to the unreasonable assumption of particle mixing state, which varies with their aging and other physiochemical processes in the atmosphere. This has been stated in the text.

Line 275: These numbers don't match the figure. With R<sup>2</sup> values of 0.01-0.23 for the  $\kappa_{\text{chem}}$  and  $\kappa_{\text{gf}}$  correlations, I would hesitate to report the slope of the fit line. Anchoring the line and a value other than (0,0) would give a different slope with a similar R<sup>2</sup> value.

Re: Yes, the reviewer is right. The discussion about the slopes and  $R^2$  has been revised

(See lines 272-280) as follows,

““...The results show that, although the slopes from linear fitting of  $\kappa_{\text{chem}}$  and  $\kappa_{\text{gf}}$  are close to 1.0, it is with quite poor correlations (typically with correlation coefficients,  $R^2$ , of  $< 0.3$ ) between  $\kappa_{\text{chem}}$  and  $\kappa_{\text{gf}}$  of the 80, 110, 150, 200 nm particles both in winter and summer. The poor correlations reflect large uncertainty in one or both of the calculated parameters that are likely due to the unreasonable assumption of particle mixing state (e.g. Cruz and Pandis, 2000; Svenningsson et al., 2006; Sjogren et al., 2007; Zardini et al., 2008), which varies with their aging and other physiochemical processes in the atmosphere. Note that underestimation of  $\kappa_{\text{chem}}$  for the summer occurred mostly in the afternoon (Marked in blue dots in Fig. 5). This may be associated with photochemical processes at around noontime. More specific investigations of the particle mixing and aging impacts on  $\kappa_{\text{chem}}$  will be further addressed in the following sections....”

Line 292: In figure 6 the gap between  $\kappa_{\text{gf}}$  and  $\kappa_{\text{chem}}$  for larger particles looks similar across all plots. A closer look that  $\kappa_{\text{chem}}$  is higher in the late afternoon only in winter, and lower in summer. But, all the error bars appear to overlap almost completely. I strongly recommend displaying the data such that the error bars can be distinguished. By way of example: the dotted lines in the background are unhelpful, the resolution of the figure is not high, and the midpoint of the error bar is not entirely necessary if the error bars are symmetric above/below this point. Some authors use overlapping shaded regions. In panel B the yellow trace is hard to see. Error bars are omitted.

Re: Thanks for the comments. The figure has been revised. As the reviewer suggested, we use shaded regions to indicate the error bar (see Fig. R2).



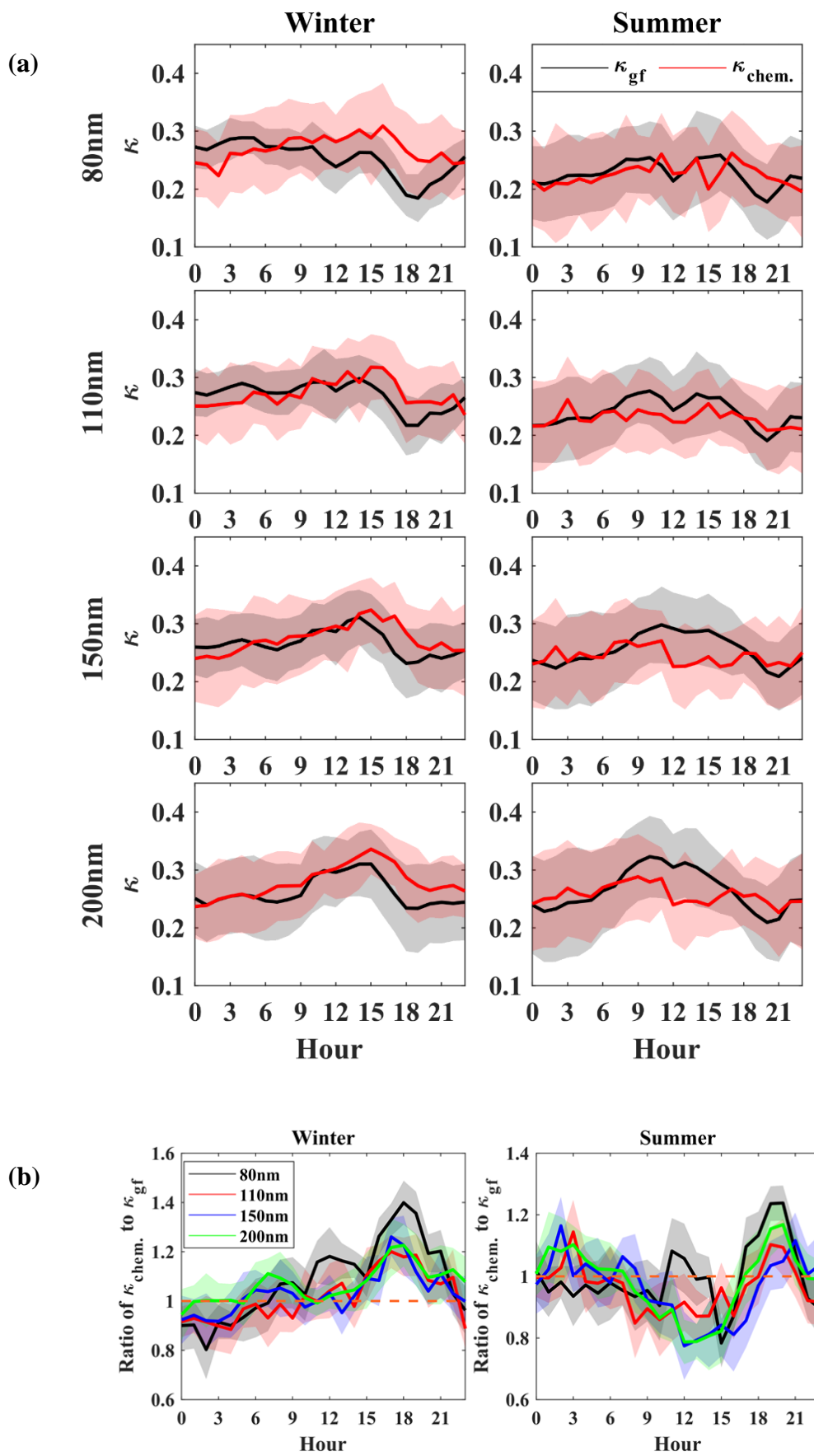


Figure R2. Diurnal variations of (a)  $\kappa_{\text{chem}}$  using size-resolved chemical composition

data and  $\kappa_{gf}$  in winter and summer period; and (b) ratio of  $\kappa_{chem}$  to  $\kappa_{gf}$  in winter and summer period. The shade regions denote the error bars ( $1\sigma$ ).

Figure S6: How is Figure S6 different from Figure 6?

Re: To examine the impacts of pollution conditions on the diurnal variations of  $\kappa$ , Figure S6 (Now Fig S1 in the revised version) shows the diurnal cycles under clean and polluted cases respectively in winter; while Fig 6 just shows an overall diurnal change of  $\kappa$  in summer and winter.

Figure S1 and others: Kappa should not be negative and this could indicate evaporation of some fraction of particles.

Re: These figures have been revised (see an example as follows, Fig. R3). But it was removed from the revised version according to reviewer's comments.

Figure R3. Mean probability density functions of hygroscopicity parameter derived from hygroscopic growth factor for 40, 80, 110, 150, 200 nm in winter and summer period respectively.

Comments on underlying physical processes

The readership may already have an understanding of internal vs external mixtures.

The description of internal vs external mixing is not succinct and does not contain many references – I suggest reducing the length of this review and incorporating the following elements: more quantitative information, more references and conclusions drawn from previous work.

Re: More previous studies and references on water uptake by mixtures of compounds have been included in the introduction, and some words about the definition of mixing state have been removed in the revised version (Lines 50-82) as follows,

“ ...The hygroscopic properties of both the natural and anthropogenic aerosols, in addition to being affected by its chemical composition (Gunthe et al., 2009), are also affected by the particle mixing state and aging (Schill et al., 2015; Peng et al., 2017). For example, a recent laboratory study shown that the coexisting hygroscopic species have a strong influence on the phase state of particles, thus affecting chemical interactions between inorganic and organic compounds as well as the overall hygroscopicity of mixed particles (Peng et al., 2016). The field measurements also demonstrated that the hydrophobic black carbon particles became hygroscopic with atmospheric mixing and aging by organics (i.e. Peng et al., 2017). In a heavily polluted atmosphere, the aerosol sources and sinks are varied, the physical and chemical processes experienced by the aerosols are complex, and the mixing state and its impact on aerosols hygroscopicity is more complicated. The hygroscopicity of mixed particles and mutual impacts between the components are still poorly understood.

Previous studies have shown that the difference between the  $\kappa$  obtained from H-TDMA or CCNc measurements and that calculated based on the volume mixing ratio of chemical components,  $\kappa_{chem}$ . Laboratory results from Cruz and Pandis (2000) indicate that  $\kappa_{gf}$  of internally mixed ammonium sulfate and organic matter is higher than  $\kappa_{chem}$  calculated for assumed uniform internal mixing. But Peng et al (2016) found that, for sodium chloride and organic aerosols mixed particles, the measured growth factors by H-TDMA were significantly lower than calculations from the mixing rule methods. In some field studies on aged aerosols, the  $\kappa$  was underestimated by the calculation based on uniform internal mixing assumption and thus lead to an underestimation of CCN concentration (Bougiatioti, et al., 2009; Chang, et al., 2007; Kuwata, et al., 2008; Wang, et al., 2010; Ren et al., 2018). However, for primary emissions dominated periods, the  $\kappa$  value from calculations based on bulk chemical composition was much higher than that measured by H-TDMA measurements (Zhang et al., 2017). The various results from previous studies suggest distinct effects of aerosols mixing state on their hygroscopicity. Overall, to what extent do the differences depend on the mixing state and the extent of aging of the particles, and how the different atmospheric processes and what kinds of mixing structure of the particles may result in those disparity between measured and calculated hygroscopic parameter have not been clearly clarified by the previous studies. A comprehensive and systematic investigation on the cause and magnitude of the effect has been lacking.

In the atmosphere, the  $\kappa$ , which is related to the particle mixing state diversity, varies largely across the size range of ambient fine particles (Rose et al., 2010). Previous study only compared the measured  $\kappa$  to that calculated based on bulk chemical composition (Zhang et al., 2017). Using size-resolved, not bulk, chemical composition measurements in different seasons is expected to provide more comprehensive understanding and insights of how the aerosols mixing state influence on their hygroscopicity, motivating our analysis that employs size-resolved chemical composition measured by an HR-ToF-AMS in this study....”

Line 53: Are they? Water uptake by coated particles (including those coated with aliphatic compounds) is likely not inhibited.

Re: This should be “.....In the case of external mixing, the chemical components in the aerosol particles are independent of each other, and the chemical composition of the different types of aerosol particles is different within a certain particle size range.”

However, we have made a through revision of the introduction part.

Line 71-73: There have been continuing studies of the hygroscopicity of mixed aerosols

under controlled conditions, which may provide additional framework for mechanistic discussion.

<https://pubs.acs.org/doi/full/10.1021/acscentsci.5b00174>

<https://agupubs.onlinelibrary.wiley.com/doi/full/10.1029/2011JD016823>

<https://agupubs.onlinelibrary.wiley.com/doi/full/10.1029/2007JD009274>

<https://pubs.acs.org/doi/10.1021/acs.jpca.5b09373>

Re: We really appreciate your comments. These studies above listed are very helpful for improving our understanding of hygroscopicity of mixed aerosols. More discussions about the effect of mixed aerosols on hygroscopicity have been included in the revised manuscript by referring these studies in both the introduction, method and the interpretation and discussion of underlying physical processes.

For example,

Lines 50-55, “The hygroscopic properties of both the natural and anthropogenic aerosols, in addition to being affected by its chemical composition (Gunthe et al., 2009), are also affected by the particle mixing state (Schill et al., 2015; Peng et al., 2017). For example, a recent laboratory study shown that the coexisting hygroscopic species have a strong influence on the phase state of particles, thus affecting chemical interactions between inorganic and organic compounds as well as the overall hygroscopicity of mixed particles (Peng et al., 2016). The field measurements also demonstrated that the .....

Lines 61-66, “Previous studies have shown that the difference between the  $\kappa$  obtained from H-TDMA

or CCNc measurements and that calculated based on the volume mixing ratio of chemical components,  $\kappa_{chem}$ . Laboratory results from Cruz and Pandis (2000) indicate that  $\kappa_{gf}$  of internally mixed ammonium sulfate and organic matter is higher than  $\kappa_{chem}$  calculated for assumed uniform internal mixing. But Peng et al (2016) found that, for sodium chloride and organic aerosols mixed particles, the measured growth factors by H-TDMA were significantly lower than calculations from the mixing rule methods. In some field studies on aged aerosols,”

Lines 184-189, “...But, different from the  $\kappa_{gf}$  measured by the HTDMA system which is operated at RH of 90%, the  $\kappa_{CCNc}$  is derived by measuring aerosols CCN activity under the condition of supersaturations with relative humidity of >100%. Previous studies from field measurements and laboratory experiments showed that the  $\kappa_{CCNc}$  is generally slight larger or smaller than  $\kappa_{gf}$ , but they are basically comparable and can well represent an overall aerosols hygroscopicity (e.g. Carrico et al., 2008; Wex et al., 2009; Good et al., 2010; Irwin et al., 2010; Cerully et al., 2011; Wu et al., 2013; Zhang et al., 2017).....”

Lines 351-355, “...Besides the impacts of BC aging (changes in morphology/density) and variations of the overall density of organics on particles hygroscopicity, uncertainty in  $\kappa_{chem}$  may be related to the uncertainty in the hygroscopic parameter for organics that could vary widely over a range of diverse constituents of SOA (Suda et al., 2012). However, Zhang et al. (2017) shown that using a smaller or larger  $\kappa_{SOA}$  could not fully explain the overestimation during traffic hours or the underestimation around noontime....”

## **Anonymous Referee #2**

In this manuscript, Fan et al. measured the hygroscopicity and chemical composition of the size-resolved aerosols at several locations in northern China, and calculated the hygroscopic parameter ( $\kappa$ ) based on both the hygroscopic growth factor from HTDMA measurement ( $\kappa_{gf}$ ) and the chemical composition from HR-AMS measurement ( $\kappa_{chem}$ ). By comparing  $\kappa_{gf}$  and  $\kappa_{chem}$ , this study demonstrates clear and undisputed evidence of possible bias in estimating aerosol hygroscopicity using the chemical mixing rule. Moreover, Fan et al. provides reasonable insight on the influence of atmosphere process and aerosol mixing state on the calculation of aerosol hygroscopicity. The manuscript is well organized and written. I will

recommend the publication of this manuscript in ACP, as long as the following comments are properly addressed. Note that comments 4-6 are just suggestions.

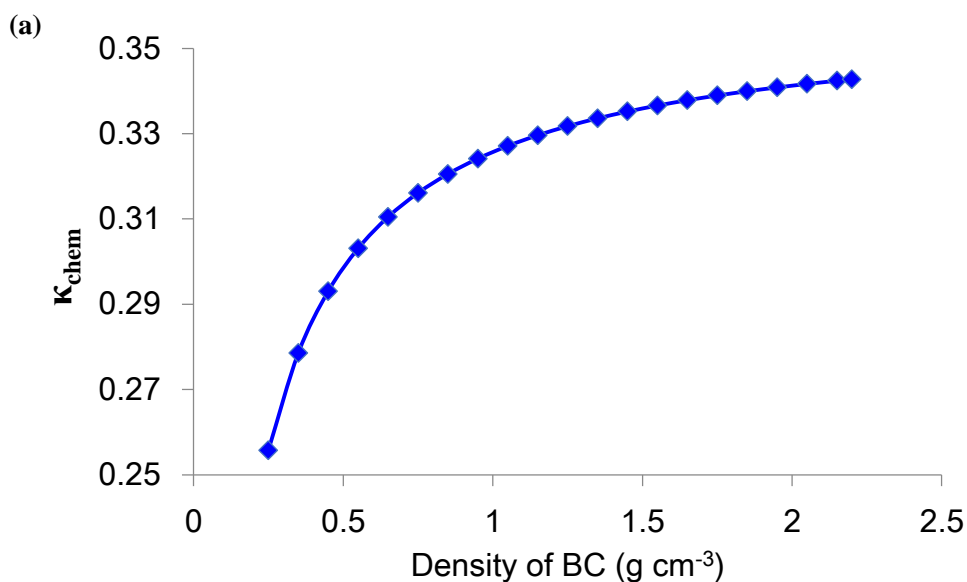
Re: We are grateful to reviewer 2 for the insightful and constructive comments and have revised our paper accordingly to account for the reviewer's recommendations.

(1) A major discovery of the paper is that  $\kappa_{\text{chem}}$  calculated using the mixing rule cannot reflect the aerosol hygroscopicity. For example, it is found that the  $\kappa_{\text{chem}}$  in summer is underestimated at noon, overestimated at late peak hours, and substantially consistent with  $k_{\text{gf}}$  at midnight. Though I think the results should be correct, I am not fully convinced by some of the interpretation. (a) Why the external mixing of BC and POA with other components during the late peak hour will result in overestimation of  $\kappa_{\text{chem}}$ ?

Re: The emission of a large number of primary hydrophobic particles like BC and POA leads to great decrease of the overall aerosol hygroscopicity. We have included discussions and statements in the revised manuscript (lines 319-346, Fig. 8) as follows (Fig. R3),

“...We suppose that the large disparity between  $\kappa_{\text{chem}}$  and  $k_{\text{gf}}$  is due to temporal variations in actual density of BC and organics caused by the particles aging and local sources. The externally-mixed BC particles are with fractal structure and chain-like aggregates and have been reported with effective density of 0.25-0.45 g cm<sup>-3</sup> (McMurry et al., 2002), While the BC particles in the calculation is assumed as void free with effective density of 1.7 g cm<sup>-3</sup>. Such inappropriate assumption would lead to an underestimation of BC volume fraction and thus the overestimation in  $\kappa_{\text{chem}}$  during the traffic rush hour and cooking time when BC particles are mostly freshly emitted with uncompacted structure. In addition, the significant increase in volume fraction of POA during the late afternoon would result in a lower density of organics, which is expected to be smaller than the assumed one (1.2 g cm<sup>-3</sup>) in the calculation. A sensitivity test has been done to examine the effect of density of BC and organics on calculated  $\kappa_{\text{chem}}$  (Fig. 7). The result shows that the  $\kappa_{\text{chem}}$  value reduces by 16-33% when applying the BC effective density of 0.25-0.45 g cm<sup>-3</sup>. This basically explains the disparity during the traffic rush hour. However, the changes in  $\kappa_{\text{chem}}$  are within  $\pm 4\%$  when changing the organic density from 1.0 (typical for POA) to 1.4 (typical for SOA) g cm<sup>-3</sup>, suggesting insensitivity of  $\kappa_{\text{chem}}$  to variations of

organic density. The result also indicates that, to fill the gap between  $\kappa_{\text{chem}}$  and  $\kappa_{\text{gf}}$  observed at noontime, the effective density of BC should be extremely high due to the decreased sensitivity of  $\kappa_{\text{chem}}$  to BC density with the aging of BC. In this case, the assumed density of BC is  $1.7 \text{ g cm}^{-3}$ , which reflects a very compacted and void free structure of the BC particles. The current applied value represents an upper limit for the effective density of ambient BC particles according to previous observations at a site near urban Beijing (Zhang et al., 2015), which suggested the aged BC is generally with effective density of  $1.2 \text{ g cm}^{-3}$ . Using this ambient observed density would lead to further underestimation in  $\kappa_{\text{chem}}$ . Our results exhibit the increase of the density of BC and organics cannot explain the disparity between  $\kappa_{\text{chem}}$  and  $\kappa_{\text{gf}}$  observed around noontime in summer. This just, on the other hand, verifies the photochemical aging/coating effect on the aerosols hygroscopicity. In addition, the coexisting hygroscopic and hydrophobic species may have a strong influence on the phase state of particles, also likely affecting chemical interactions between inorganic and organic compounds as well as the overall hygroscopicity of mixed particles (Peng et al., 2016). Further investigations are needed to verify this. Our study suggest that, to accurately parameterize the effect of BC aging on particles hygroscopicity, future investigations need to measure the effective density and morphology of ambient BC, in particularity in those regions with complex local sources.....”



(b)

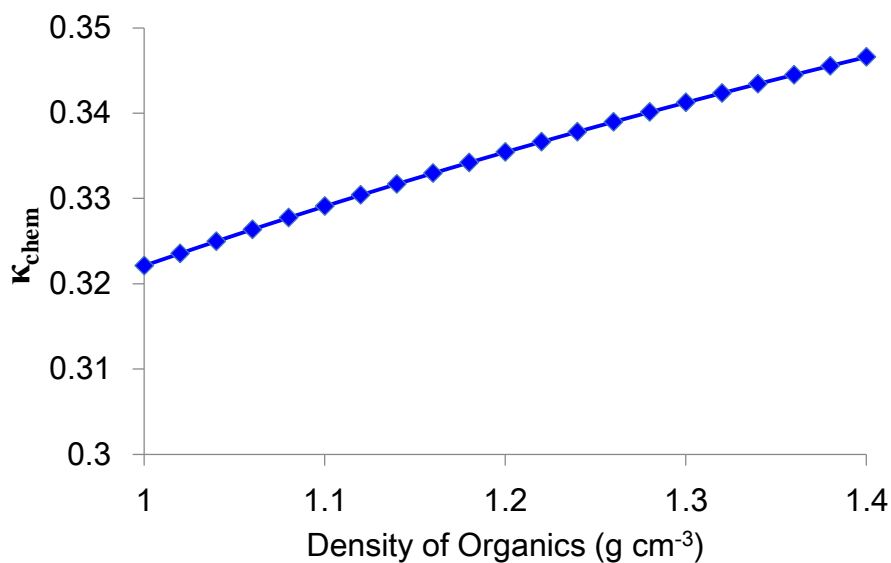


Figure R3. Sensitivity of  $\kappa_{chem}$  to variations of density of BC (a) and organics (b)

(b) According to the author’s argument, aerosols both at noon and at midnight have core-shell structure, but why the  $\kappa_{chem}/k_{gf}$  is quite distinct? More detailed interpretation and discussion are necessary.

Re: At noontime, the rapid photochemical aging of BC particles leads to the core-shell structure in which certain secondary aerosol generated from photochemical reactions is thickly coated on the surface of BC. However, the condensation effect during nighttime is less significant (indicated by the smaller disparity between  $\kappa_{chem}$  and  $\kappa_{gf}$ ) than the coating effect caused by aerosols photochemical aging at noontime, due to thinner coating layer formed on the pre-exist particles during nighttime or other factors influencing the particles hygroscopicity. We have included a statement in the revised manuscript (see lines 367-373) as follows,

“...We propose the increased underestimation during polluted conditions is likely due to enhanced condensation of secondary hygroscopic compounds (e.g. nitrate, sulfate) on pre-existing aerosols at lower temperature and higher relative humidity at nighttime (Wu et al., 2008; Wang et al., 2016; An et al., 2019). However, such condensation effect during nighttime is less significant



(indicated by the smaller disparity between  $\kappa_{chem}$  and  $\kappa_{gf}$ ) than the coating effect caused by aerosols photochemical aging at noontime, likely due to thinner coating layer formed on the pre-exist particles during nighttime or other factors influencing the particles hygroscopicity....”

(2) L259, “Since a size-resolved BC mass concentration measurement was not available during the campaign, we use the bulk mass fraction of BC particles measured by the AE33 combining with size-resolved BC distribution in Beijing reported by Liu et al. (2018) to estimate  $\kappa_{chem}$ .” As far as I know, the instrument to measure the size distribution of BC in Liu et al. (2018) is a SP2, which gives the BC core diameter. It is necessary to explain how to convert this size distribution of BC core to the size distribution of ambient aerosols.

Re: We have provided a statement in the revised version as following (also see lines 260 -263),

“...During the calculation, the BC core diameter measured by SP2 has been converted to the diameter of coated BC particles by multiplying factors of 1.4 and 2.6 under clean (with bulk BC mass concentrations  $<2 \mu\text{g m}^{-3}$ ) and polluted (with bulk BC mass concentrations  $>2 \mu\text{g m}^{-3}$ ) conditions respectively (Liu et al., 2018). ...”

(3) L227 and fig. 3. “the concentration of the hydrophilic mode increased quickly around noontime and in the early afternoon (12:00-16:00)”, which is explained by a transformation of the particles from externally to internally mixing state. However, I have different opinion. From Fig. 3a, it is evident that 40 nm particles after 12:00 were dominated by new particle formation (NPF). Therefore, the decrease of hydrophobic mode could be attribute to the extremely large amount of hydrophilic particles from NPF overwhelmed all other particles.

Re: Thanks a lot for the comments. We have revised and included an explanation of

“In addition, it is evident that 40 nm particles after 12:00 were dominated by NPF (Fig. 3). Therefore, the increase of hydrophobic mode particles suggests that a large

amount of hydrophilic particles are generated from NPF.” in the revised manuscript (see lines 220-222).

(4) It will be better if the authors can discuss more on the similarities and differences of the hygroscopicity calculation at different sites.

Re: We have provided more details on clarify how we derive and calculate the particles hygroscopicity at different sites (lines 179-189) as follows,

“...In addition, we also compare the results from the field campaigns with those from other two sites, Xingtai (XT: 37.18 °N, 114.37 °E), and Xinzhou (XZ: 38.24 °N, 112.43 °E), in North China Plain (Fig. 1). At XZ site, we use the hygroscopic parameter (defined as  $\kappa_{CCNc}$ ) from size-resolved CCN measurements (Zhang et al., 2014, 2016) for comparison. More detailed descriptions of the method to retrieve  $\kappa_{CCNc}$  can be found in (Petters and Kreidenweis (2007)). Both of the  $\kappa_{gf}$  and  $\kappa_{CCNc}$  are derived based on  $\kappa$ -Köhler Theory (Petters and Kreidenweis, 2007). But, different from the  $\kappa_{gf}$  measured by the HTDMA system which is operated at RH of 90%, the  $\kappa_{CCNc}$  is derived by measuring aerosols CCN activity under the condition of supersaturations with relative humidity of >100%. Previous studies from filed measurements and laboratory experiments showed that the  $\kappa_{CCNc}$  is generally slight larger or smaller than  $\kappa_{gf}$ , but they are basically comparable and can well represent an overall aerosols hygroscopicity (e.g. Carrico et al., 2008; Wex et al., 2009; Good et al., 2010; Irwin et al., 2010; Cerully et al., 2011; Wu et al., 2013; Zhang et al., 2017).”

(5) There have been several studies revealing the uncertainty of calculating hygroscopicity using the mixing rule, but few can provide proper solution. Is it possible for the authors to propose parameterized modification on the  $\kappa_{chem}$  to reduce the uncertainty? If so, this paper will be enormously improved and will be far distinct from other studies. For example, should we use lower BC density value during the rush hours?

Re: This is a good point. We have made a sensitivity test to examine the effect of density of BC on calculated  $\kappa_{chem}$ , and included statements and discussions about this in the revised version (lines 319-346, Fig. 8) as follows (Fig. R4),

“...We suppose that the large disparity between  $\kappa_{chem}$  and  $\kappa_{gf}$  is due to temporal variations in actual density of BC and organics caused by the particles aging and local sources. The externally-mixed BC

particles are with fractal structure and chain-like aggregates and have been reported with effective density of 0.25-0.45 g cm<sup>-3</sup> (McMurry et al., 2002). While the BC particles in the calculation is assumed as void free with effective density of 1.7 g cm<sup>-3</sup>. Such inappropriate assumption would lead to an underestimation of BC volume fraction and thus the overestimation in  $\kappa_{chem}$  during the traffic rush hour and cooking time when BC particles are mostly freshly emitted with uncompacted structure. In addition, the significant increase in volume fraction of POA during the late afternoon would result in a lower density of organics, which is expected to be smaller than the assumed one (1.2 g cm<sup>-3</sup>) in the calculation. A sensitivity test has been done to examine the effect of density of BC and organics on calculated  $\kappa_{chem}$  (Fig. 7). The result shows that the  $\kappa_{chem}$  value reduces by 16-33% when applying the BC effective density of 0.25-0.45 g cm<sup>-3</sup>. This basically explains the disparity during the traffic rush hour. However, the changes in  $\kappa_{chem}$  are within  $\pm 4\%$  when changing the organic density from 1.0 (typical for POA) to 1.4 (typical for SOA) g cm<sup>-3</sup>, suggesting insensitivity of  $\kappa_{chem}$  to variations of organic density. The result also indicates that, to fill the gap between  $\kappa_{chem}$  and  $\kappa_{gf}$  observed at noontime, the effective density of BC should be extremely high due to the decreased sensitivity of  $\kappa_{chem}$  to BC density with the aging of BC. In this case, the assumed density of BC is 1.7 g cm<sup>-3</sup>, which reflects a very compacted and void free structure of the BC particles. The current applied value represents an upper limit for the effective density of ambient BC particles according to previous observations at a site near urban Beijing (Zhang et al., 2015), which suggested the aged BC is generally with effective density of 1.2 g cm<sup>-3</sup>. Using this ambient observed density would lead to further underestimation in  $\kappa_{chem}$ . Our results exhibit the increase of the density of BC and organics cannot explain the disparity between  $\kappa_{chem}$  and  $\kappa_{gf}$  observed around noontime in summer. This just, on the other hand, verifies the photochemical aging/coating effect on the aerosols hygroscopicity. In addition, the coexisting hygroscopic and hydrophobic species may have a strong influence on the phase state of particles, also likely affecting chemical interactions between inorganic and organic compounds as well as the overall hygroscopicity of mixed particles (Peng et al., 2016). Further investigations are needed to verify this. Our study suggest that, to accurately parameterize the effect of BC aging on particles hygroscopicity, future investigations need to measure the effective density and morphology of ambient BC, in particularity in those regions with complex local sources.....”

(6) For several times, the current manuscript cited Zhang et al. (2017), which is one of the previous studies done by the same group on the same topic. Therefore, it is appropriate to make a clear statement of the unresolved issues in the previous paper or what improvement has been made to this study so that the reader can easily understand the novelty of this paper.

Re: We have included the following statement in the revised version (also see lines 77-82),

“...In the atmosphere, the  $\kappa$ , which is related to the particle mixing state diversity, varies largely across the size range of ambient fine particles (Rose et al., 2010). Previous study only compared the

measuredkto that calculated based on bulk chemical composition (Zhang et al., 2017). Using size-resolved, not bulk, chemical composition measurements in different seasons is expected to provide more comprehensive understanding and insights of how the aerosols mixing state influence on their hygroscopicity, motivating our analysis that employs size-resolved chemical composition measured by an HR-ToF-AMS in this study.”

Other minor comments:

(1) fig. 2 is not reader-friendly. Please work out some way to make the information more clear.

Re: Revised.

(2) fig.3. There are totally 12 sub-figures here. Please consider naming each sub-figures rather than the current way (which is not clearly demonstrated).

Re: Revised.

(3) L150 and L160, the full term and the abbreviations of probability density functions (PDF) should be provided the first time in the text.

Re: Revised.

(4) Fig. 5, L266, should be “slopes of linear fits and correlation coefficients”.

Re: Revised.

1 **Contrasting ambient fine particles hygroscopicity derived by HTDMA and HR-AMS measurements**  
2 **between summer and winter in urban Beijing**

3 Xinxin Fan<sup>1</sup>, Jieyao Liu<sup>1</sup>, Fang Zhang<sup>1\*</sup>, Lu Chen<sup>1</sup>, Don Collins<sup>2</sup>, Weiqi Xu<sup>3,4</sup>, Xiaoi Jin<sup>1</sup>, Jingye  
4 Ren<sup>1</sup>, Yuying Wang<sup>1,5</sup>, Hao Wu<sup>1</sup>, Shangze Li<sup>1</sup>, Yele Sun<sup>3,4</sup>, Zhanqing Li<sup>1,6</sup>

5  
6 <sup>1</sup>State Key Laboratory of Earth Surface Processes and Resource Ecology, College of Global Change and  
7 Earth System Science, Beijing Normal University, Beijing 100875, China

8 <sup>2</sup>Department of Chemical and Environmental Engineering, University of California Riverside, Riverside,  
9 California, USA

10 <sup>3</sup>State Key Laboratory of Atmospheric Boundary Layer Physics and Atmospheric Chemistry, Institute of  
11 Atmospheric Physics, Chinese Academy of Sciences, Beijing 100029, China

12 <sup>4</sup>College of Earth Sciences, University of Chinese Academy of Sciences, Beijing 100049, China

13 <sup>5</sup>School of Atmospheric Physics, Nanjing University of Information Science and Technology, Nanjing  
14 210044, China

15 <sup>6</sup>Earth System Science Interdisciplinary Center and Department of Atmospheric and Oceanic Science,  
16 University of Maryland, College Park, Maryland, USA

17  
18 Correspondence to: [Fang.zhang@bnu.edu.cn](mailto:Fang.zhang@bnu.edu.cn)

19 **Abstract**

20 The effects of aerosols on visibility through scattering and absorption of light and on climate through  
21 altering cloud droplet concentration are closely associated with their hygroscopic properties. Here, based on  
22 field campaigns in winter and summer in Beijing, we compare the size-resolved hygroscopic parameter ( $\kappa_{gf}$ )  
23 of ambient fine particles derived by an HTDMA (Hygroscopic Tandem Differential Mobility Analyzer) to  
24 that (denoted as  $\kappa_{chem}$ ) of calculated by an HR-ToF-AMS (High-resolution Time-of-Flight Aerosol Mass  
25 Spectrometer) measurements using a simple rule with a uniform internal mixing hypothesis. We mainly  
26 focus on contrasting the disparity of  $\kappa_{gf}$  and  $\kappa_{chem}$  between summer and winter to reveal the impact of  
27 atmospheric processes/sources on aerosols hygroscopicity and to evaluate the uncertainty in estimating  
28 particles hygroscopicity with the hypothesis. We show that, in summer, the  $\kappa_{chem}$  for 110, 150 and 200 nm  
29 particles was averagely ~10% - 12% lower than  $\kappa_{gf}$ , with the greatest difference between the values observed  
30 around noontime when aerosols experience rapid photochemical aging. In winter, no apparent disparity  
31 between  $\kappa_{chem}$  and  $\kappa_{gf}$  is observed for those >100 nm particles around noontime, but the  $\kappa_{chem}$  is much higher  
32 than  $\kappa_{gf}$  in the late afternoon when ambient aerosols are greatly influenced by local traffic and cooking

33 sources. By comparing with the observation from other two sites (Xingtai, Hebei and Xinzhou, Shanxi) of  
34 north China, we verify that atmospheric photochemical aging of aerosols enhances their hygroscopicity and  
35 may induce a coating effect which thereby leads to 10%-20% underestimation of the hygroscopic parameter  
36 if using the uniform internal mixing assumption. The coating effect is found more significant for these >100  
37 nm particles observed in remote or clean regions. However, local primary sources, which result in ~~an~~  
38 ~~externally mixture of the fine particles with~~ a large number of externally-mixed BC and POA (Primary  
39 Organic Aerosol) in urban Beijing, ~~makes the particle much less hygroscopic and during traffic rush hour~~  
40 time, cause 20-40% overestimation of the hygroscopic parameter. This is largely due to an inappropriate use  
41 of density of the BC that is closely associated with its morphology, and the results show that the calculation  
42 can be improved by applying an effective density of freshly BC within the range of 0.25-0.45 g cm<sup>-3</sup> in the  
43 mixing rule assumption. In addition, we also note lower  $\kappa_{chem}$  than  $\kappa_{eff}$  for 80, 110 and 150 nm particles  
44 during the nighttime of winter, particularly in polluted days, probably due to a nighttime coating effect  
45 driven by condensation of secondary hygroscopic species on pre-existing aerosols in cold season. Our  
46 results study suggest that it is critical to measure the effective density and morphology of ambient BC in  
47 particularity in those regions with complex local sources, so as to accurately parameterize the impacts in  
48 model simulations to improve the evaluation of the aerosols indirect effect. effect of BC aging on particles  
49 hygroscopicity.

带格式的: 字体颜色: 文字 1, 英语(美国)

带格式的: 字体颜色: 文字 1, 英语(美国)

带格式的: 字体颜色: 文字 1, 英语(美国)

## 50 1. Introduction

51 The effects of aerosols on visibility through scattering and absorption of light and on climate through  
52 altering cloud droplet concentration are influenced by their hygroscopic growth. Understanding and  
53 reducing the uncertainty in prediction of the aerosol hygroscopic parameter ( $\kappa$ ) using chemical composition  
54 would improve model predictions of aerosol effects on clouds and climate.

55 ~~The hygroscopic parameter,  $\kappa$ , is dependent upon particle chemical composition (Gunthe et al., 2009).~~  
56 ~~The~~ The hygroscopic properties of ~~an aerosol~~ both the natural and anthropogenic aerosols, in addition to  
57 being affected by its chemical composition, (Gunthe et al., 2009), are also affected by the particle mixing  
58 state and aging (Schill et al., 2015; Peng et al., 2017). ~~The mixing~~ For example, a recent laboratory study

带格式的

59 shown that the coexisting hygroscopic species have a strong influence on the phase state of aerosol particles  
60 can be divided into external mixing and internal mixing. The chemical components in the aerosol, thus  
61 affecting chemical interactions between inorganic and organic compounds as well as the overall  
62 hygroscopicity of mixed particles are independent of each other. The chemical composition of the different  
63 types of aerosol (Peng et al., 2016). The field measurements also demonstrated that the hydrophobic black  
64 carbon particles is different within a certain particle size range, and the mixed state is external mixing. As  
65 the aerosol particles undergo transport, coagulation, and aging/coating in the atmosphere, the chemical  
66 components become more uniformly mixed within each particle size range, became hygroscopic with the  
67 aerosol mixing state approaching an internal mixture. Depending on the physical properties of the different  
68 aerosol components, internal mixing can be divided into uniform internal atmospheric mixing and “core-shell”  
69 mixing (Jacobson, 2001). For uniform internal mixing the distribution of the chemical components is the  
70 same throughout each particle. “Core-shell” mixing refers to a mixing state in which certain chemical  
71 components are coated or coagulated on the surface of other chemical components (such as black carbon)  
72 during aging by organics (i.e. Peng et al., 2017). In the heavily polluted atmosphere, the aerosol sources  
73 and sinks are varied, the physical and chemical processes experienced by the aerosols are complex, and the  
74 mixing state and its impact on aerosols hygroscopicity is more complicated. In heavily polluted areas, BC is  
75 usually mixed with other chemical components. Freshly emitted BC is mostly in an external mixed state.  
76 With the aging process, it gradually transforms into the internal mixing state (Chen, et al., 2016; Lee, et al.,  
77 2015; Wang, The hygroscopicity of mixed particles and mutual impacts between the components are still  
78 poorly understood, et al., 2017). Based on observations in the winter of Beijing urban area, Wang et al. (2019)  
79 found that the secondary aerosol generated from photochemical reactions is thickly coated on the surface of  
80 BC.

81 Studies Previous studies have shown that the difference between the  $\kappa$  obtained using from H-TDMA  
82 data,  $\kappa_{gf}$  or CCNc measurements and that calculated based on the volume mixing ratio of chemical  
83 components,  $\kappa_{chem}$ , depends on the mixing state and the extent of aging of the particles (Mikhailov, et al.,  
84 2015; Zhang et al., 2017). Results. Laboratory results from Cruz and Pandis (2000) also indicate that  $\kappa_{gf}$  of  
85 internally mixed ammonium sulfate and organic matter is higher than  $\kappa_{chem}$  calculated for assumed uniform

带格式的

带格式的: 字体颜色: 文字 1, 英语(美国)

86 internal mixing. ~~Similarly, in~~ But Peng et al (2016) found that, for sodium chloride and organic aerosols  
87 ~~mixed particles, the measured growth factors by H-TDMA were significantly lower than calculations from~~  
88 ~~the mixing rule methods. In some field studies on aged aerosols, the  $\kappa$  was underestimated by the~~  
89 ~~calculation based on uniform internal mixing assumption and thus lead to an underestimation of CCN~~  
90 ~~concentration~~(Bougiatioti, et al., 2009; Chang, et al., 2007; Kuwata, et al., 2008; Wang, et al., 2010), ~~the~~  
91 ~~concentration of CCN was underestimated by the calculation based on uniform internal mixing. Our~~  
92 ~~previous study demonstrated that particle mixing state has large impacts on prediction of CCN concentration~~  
93 ~~for the aerosol sampled in Beijing (Ren et al., 2018); Ren et al., 2018). However, for primary emissions~~  
94 ~~dominated periods, the  $\kappa$  value from calculations based on bulk chemical composition was much higher than~~  
95 ~~that measured by H-TDMA measurements (Zhang et al., 2017). The various results from previous studies~~  
96 ~~suggest distinct effects of aerosols mixing state on their hygroscopicity. Overall, to what extent do the~~  
97 ~~differences depend on the mixing state and the extent of aging of the particles, and how the different~~  
98 ~~atmospheric processes and what kinds of mixing structure of the particles may result in those disparity~~  
99 ~~between measured and calculated hygroscopic parameter have not been clearly clarified by the previous~~  
100 ~~studies. A comprehensive and systematic investigation on the cause and magnitude of the effect has been~~  
101 ~~lacking.~~

102 In the atmosphere, the  $\kappa$ , which is related to the particle mixing state diversity, varies largely across  
103 the size range of ambient fine particles (Rose et al., 2010). Previous study only compared the measured  $\kappa$  to  
104 that calculated based on bulk chemical composition (Zhang et al., 2017). ~~(2017) observed an evident~~  
105 ~~underestimation of around noontime particle hygroscopicity based on~~ Using size-resolved, not bulk,  
106 ~~chemical composition measurements in urban Beijing. Wang et al. (2018a) also noted a lower hygroscopic~~  
107 ~~parameter estimated by the simple volume mixing ratio than that derived from direct HTDMA measurement~~  
108 ~~at a site in North China Plain. These studies have revealed the uncertainty in the estimation of aerosol~~  
109 ~~hygroscopicity parameters using chemical composition volume mixing ratios with the assumption that of~~  
110 ~~uniform internal mixing, but there is still lack of a systematic investigation on the cause and magnitude of~~  
111 ~~the effect. Furthermore, most studies that have been conducted compare the size-resolved hygroscopic~~

带格式的

带格式的



~~parameter  $\kappa$  obtained with an HTDMA with  $\kappa$  calculated from bulk chemical composition measurements~~ different seasons is expected to provide more comprehensive understanding and insights of how the aerosols mixing state influence on their hygroscopicity, motivating our analysis that employs size-resolved chemical composition measured by an HR-ToF-AMS.

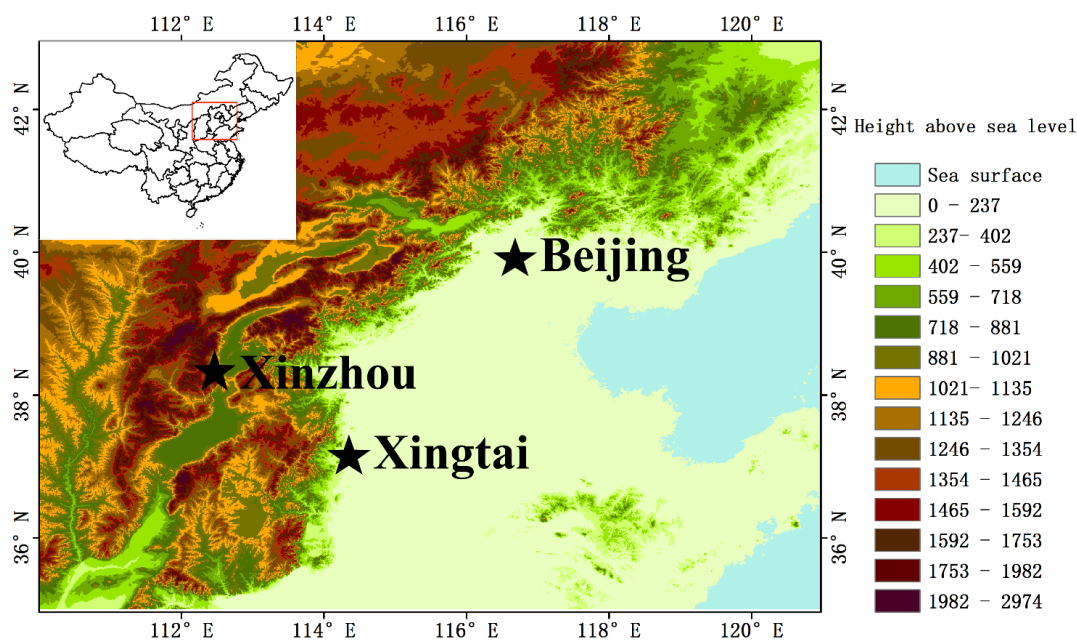
in this study. The aim of this paper is to study the hygroscopicity and mixing state characteristics of fine particles in the Beijing urban area, and to reveal the impact of atmospheric processes/sources and mixing/aging on aerosols hygroscopicity and elucidate the uncertainty in calculating the hygroscopic parameter using simple mixing rule estimates based on size-resolved chemical composition. The experiment and theory in the study are introduced in Sect. 2. The comparison between the hygroscopic parameter obtained from the HTDMA and that calculated using size-resolved chemical composition is discussed in Sect. 3. Conclusions from the study are given in Sect. 4.

## 2. Experiment and Theory

### 2.1. Site and instruments

~~In this study, we mainly focus on analysis of the data obtained from two campaigns in urban Beijing (BJ: 39.97°N, 116.37°E). In addition, we also compare the results from the field campaigns with those from two sites, Xingtai (XT: 37.18°N, 114.37°E), and Xinzhou (XZ: 38.24°N, 112.43°E), in North China Plain (Fig. 1). Two field campaigns are conducted during winter 2016 and summer 2017 of urban Beijing (Fig. 1, BJ: 39.97°N, 116.37°E) for measurements of aerosols physical and chemical properties.~~ The BJ site is located at the Institute of Atmospheric Physics (IAP), Chinese Academy of Sciences, which is between the north third and fourth ring roads in northern Beijing. Local traffic and cooking emissions can be important at the site (Sun et al., 2015). The sampling period in cold season was from 16 November to 10 December 2016, during the domestic heating period in Beijing. The sampling period in warm season was from 25 May to 18 June 2017. ~~The XT site is located in the National Meteorological Basic Station, which is about 17 km from the XT urban area. The sampling period was from 17 May to 14 June 2016. Xingtai, with a high level of industrialization and urbanization, is located in the center of the North China Plain. Due to~~

137 industrial emissions and typically weak ventilating winds, concentrations of  $PM_{2.5}$ , black carbon and gaseous  
138 precursors are extremely high at the Xingtai site (Fu et al., 2014). Xinzhou is located north of Taiyuan and  
139 about 360 km southwest of Beijing, in the north central part of Shanxi Province, and is surrounded by  
140 mountains on three sides. The XZ site is located in a town, surrounded by agricultural land (such as corn  
141 fields). Local emissions from motor vehicles and industrial activities have relatively little influence on the  
142 sampled aerosol (Zhang et al., 2016). Because of its location and elevation, the aerosol at the XZ site is  
143 usually aged and transported from other areas. The sampling period was from July 22 to August 26, 2014 at  
144 XZ site.



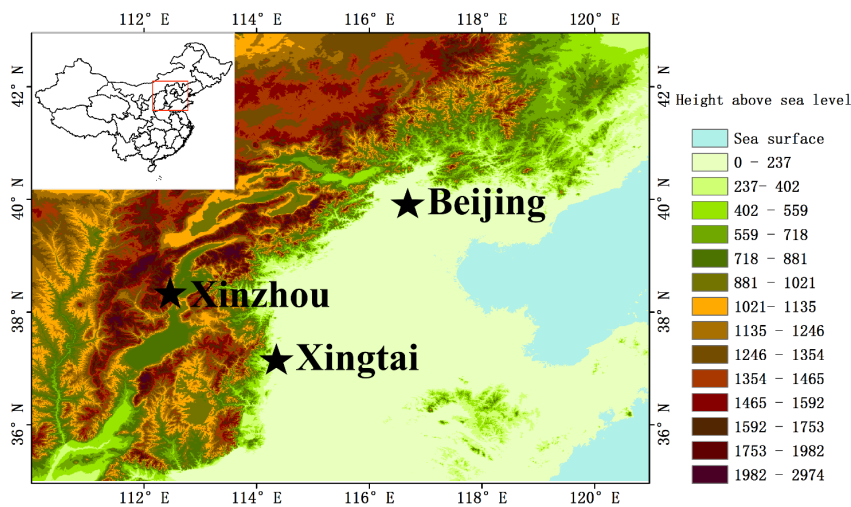


Figure 1. The map location of the sites

Particle number size distribution (PNSD) in the size range from 10 nm to 550 nm was measured with a Scanning Mobility Particle Sizer (SMPS; Wang & Flagan, 1990; Collins et al., 2002), which consists of a long differential mobility analyzer (DMA, model 3081L, TSI Inc) to classify the particle and a condensation particle counter (CPC, model 3772, TSI Inc.) to detect the size classified particles. The sampled particles were dried to relative humidity < 30% before entering the DMA. The measurement time for each size distribution was five minutes.

The HTDMA system used in this study has been described in detail in previous publications (Tan et al., 2013; Wang et al., 2017; Zhang et al., 2017). Here, only a brief description is given. A Nafion dryer dried the sampled particles to relative humidity < 20%, after which the steady state charge distribution was reached in a bipolar neutralizer. The first differential mobility analyzer (DMA<sub>1</sub>, model 3081L, TSI Inc.) selected the quasi-monodisperse particles through applying a fixed voltage. The dry diameters selected in this study were 40, 80, 110, 150, and 200 nm. The quasi-monodisperse particles were humidified to a controlled RH (90% in this study) using a Nafion humidifier. A second DMA (DMA<sub>2</sub>, same model as the DMA<sub>1</sub>) coupled with a water-based condensation particle counter (WCPC, model 3787, TSI Inc.) measured

163 the particle number size distributions of the humidified aerosol. RH calibration with ammonium sulfate was  
164 carried out regularly during the study.

165 The hygroscopic growth factor (Gf) is defined as the ratio of the mobility diameter at a given RH to the  
166 dry diameter:

$$Gf = \frac{D(RH)}{D(dry)}$$

167 The Gf probability density function (PDF) is retrieved based on the TDMA<sub>inv</sub> algorithm developed by  
168 Gysel et al. (2009). Dry scans in which the RH between the two DMAs was not increased were used to  
169 define the width of the transfer function.

170 Size-resolved non-refractory submicron aerosol composition was measured with an Aerodyne  
171 high-resolution time-of-flight aerosol mass spectrometer (HR-ToF-AMS; Xu et al., 2015). The particle  
172 mobility diameter was estimated by dividing the vacuum aerodynamic diameter from the AMS  
173 measurements by particle density. Because the uncertainty caused by the fixed density across the size range  
174 is negligible (Wang et al. 2016), here, the particle density is assumed to be 1600 kg m<sup>-3</sup> (Hu et al., 2012).  
175 AMS positive matrix factorization (PMF) with the PMF2.exe (v4.2) method was performed to identify  
176 various factors of organic aerosols. Xu et al. (2015) have described the operation and calibration of the  
177 HR-ToF-AMS in detail. Black carbon (BC) mass concentration was derived from measurements of light  
178 absorption with a 7-wavelength aethalometer (AE33, Magee Scientific Corp.; Zhao et al., 2017).

## 179 2.2. Data

180 The time series of the submicron particle mass concentration PM<sub>1</sub>, ~~(Fig. 2a),~~ bulk mass concentrations  
181 of the main species in PM<sub>1</sub> ~~(Fig. 2b),~~ mass fraction of the chemical composition of PM<sub>1</sub> ~~(Fig. 2c),~~ and  
182 probability density function of growth factor (Gf-PDFs) for 40, ~~80, 110, and~~ 150, ~~200~~ nm particles ~~(Fig.~~  
183 ~~2d-h)~~ during the campaign are presented in Fig. 2. ~~As shown in Fig. 2, quite~~ Quite distinct temporal  
184 variability of aerosol chemical and physical properties was observed between winter and summer. The  
185 average mass concentration of PM<sub>1</sub> was 55.2 µg/m<sup>3</sup> in the winter and 16.5 µg/m<sup>3</sup> in the summer during our  
186 study periods. In this study, we define the conditions when the mass concentration in winter period was < 20

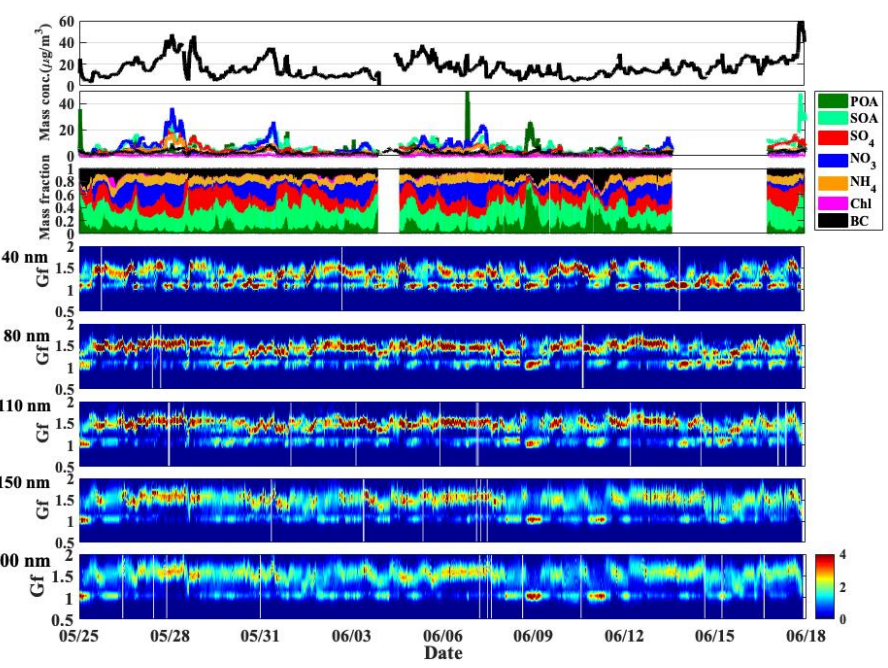
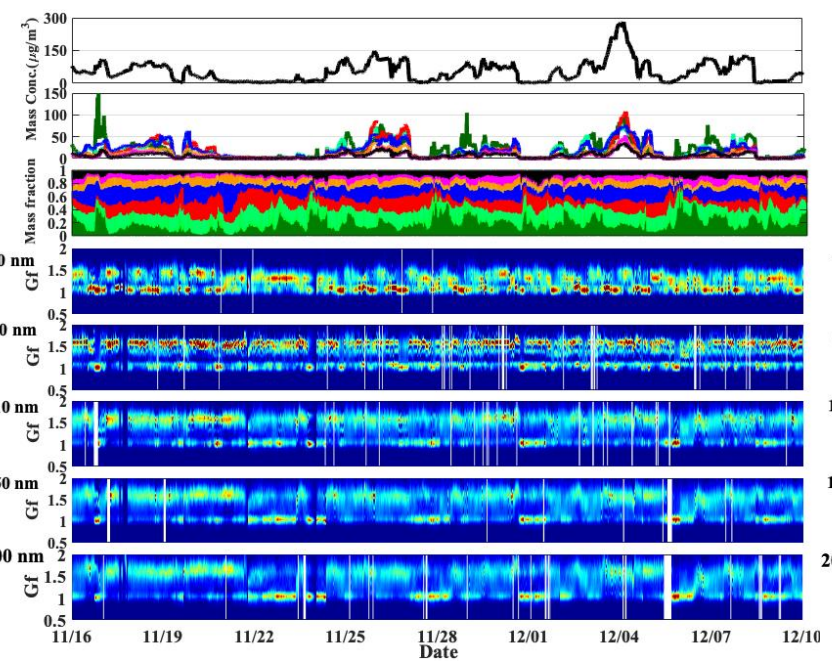
187  $\mu\text{g m}^{-3}$  and  $>80 \mu\text{g m}^{-3}$  as clean and polluted conditions, respectively. Organic aerosol (OA), consisting of  
188 secondary organic aerosol (SOA) and primary organic aerosol (POA), was the major fraction during both the  
189 winter and summer sampling periods. POA concentration was higher than that of SOA in the winter, which  
190 reflects the influence of primary emissions such as coal combustion OA (COOA) in Beijing (Hu et al., 2016;  
191 Sun et al., 2016). In contrast, SOA usually dominated in the summer, which is ~~evideneee~~evident that  
192 secondary aerosol formation played a key role in the source of  $\text{PM}_{10}$ . ~~Figs. 2d-h show the time-series of the~~  
193 ~~probability density functions (PDFs) of Gf for 40, 80, 110, 150, and 200 nm particles, respectively.~~ Distinct  
194 hydrophobic (with Gf of  $\sim 1.0$ ) and more hygroscopic (with Gf of  $\sim 1.5$ ) modes were observed from Gf-PDFs  
195 of both small and large particles. Sometimes the more hygroscopic mode particles were more concentrated  
196 and at others the hydrophobic particles were. In general though, the more hygroscopic mode dominated for  
197 larger particles (i.e. ~~150-and-200~~ nm), and the less hygroscopic mode did for the smallest particles (e.g. 40  
198 nm) ~~(Fig. 2d-h and Fig. S1)~~. Occasionally, only the hydrophobic mode was evident for ~~150-and-200~~ nm  
199 particles, which occurred when POA dominated the  $\text{PM}_{10}$ . Only the hygroscopic mode was discernable for 40  
200 nm particles during new particle formation (NPF) events that occurred more frequently in summer than  
201 winter (Fig. ~~S23~~).

202

Winter

Summer

(h)  
(f)  
(g)  
(a)  
(b)  
(c)  
(d)  
(e)



203

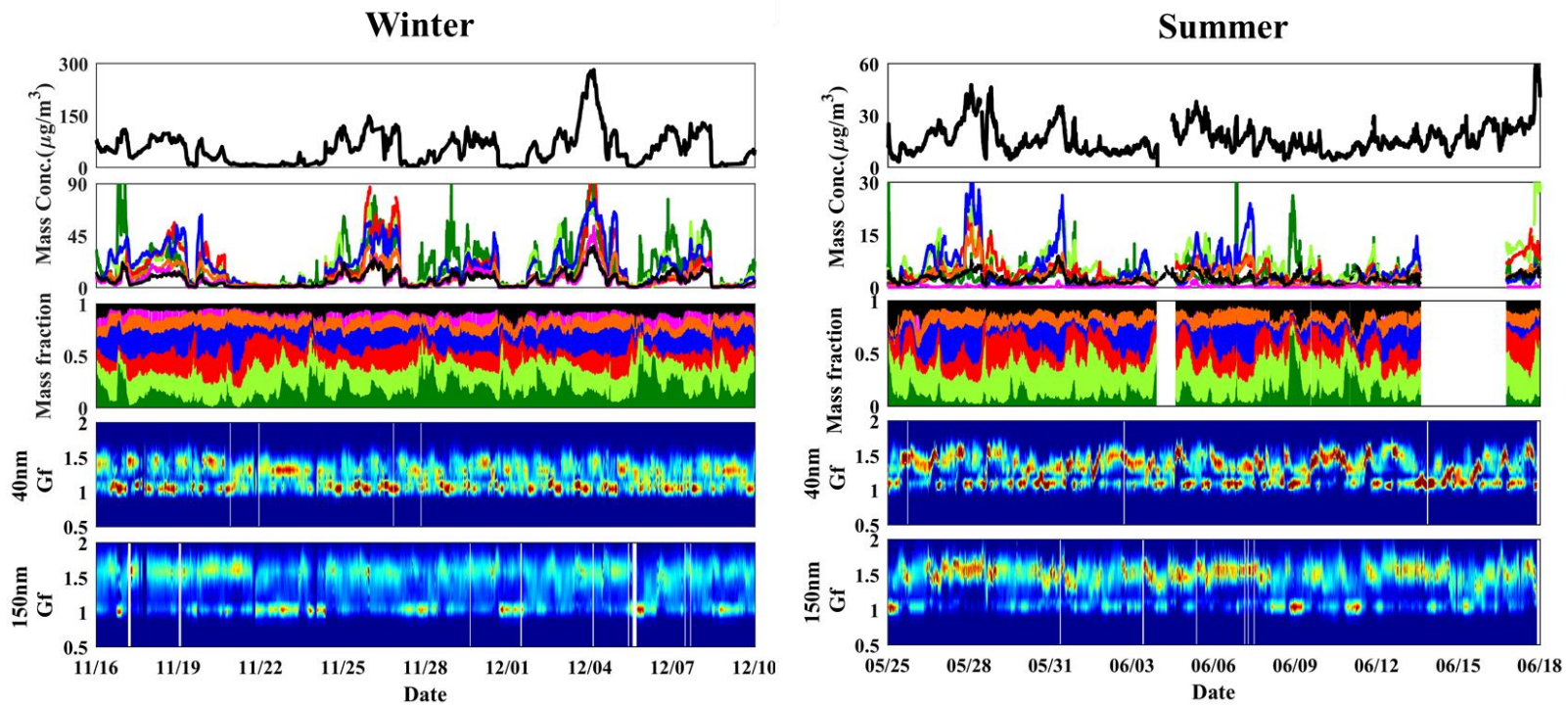


Figure 2. – Winter (left) and summer (right) time series of (a) mass concentration of  $PM_{1+2}$ ; (b) bulk mass concentration of the main species in  $PM_{1+2}$ ; (c) mass fraction of the chemical composition of  $PM_{1+2}$ ; (d-h)  $PM_{1+2}$  and Gf-PDFs for 40-, 80-, 110-, and 150 and 200-nm particles.

带格式的: 下标

带格式的: 下标

## 2.3. Theory and method

### 2.3.1 Derivation of the hygroscopic parameter, $\kappa$ , from the growth factor (Gf)

According to  $\kappa$ -Köhler Theory (Petters and Kreidenweis, 2007), the hygroscopicity parameter  $\kappa$  can be derived using the growth factor measured by an HTDMA.

$$\kappa = (Gf^3 - 1) \left( \frac{\exp\left(\frac{A}{D_d Gf}\right)}{RH} - 1 \right), \quad (1)$$

$$A = \frac{4\sigma_{s/a} M_w}{RT \rho_w}, \quad (2)$$

where Gf is hygroscopic growth factor measured by HTDMA,  $D_d$  is the dry diameter of the particles, RH is the relative humidity in the HTDMA (90%, in our study),  $\sigma_{s/a}$  is the surface tension of the solution/air (assumed here to be the surface tension of pure water,  $\sigma_{s/a} = 0.0728 \text{ N m}^{-2}$ ),  $M_w$  is the molecular weight of water, R is the universal gas constant, T is the absolute temperature, and  $\rho_w$  is the density of water.

### 2.3.2 Derivation of the hygroscopic parameter, $\kappa$ , from chemical composition data

For an assumed internal mixture,  $\kappa$  can also be calculated by a simple mixing rule on the basis of chemical volume fractions (Petters and Kreidenweis, 2007; Gunthe et al., 2009):

$$\kappa_{chem} = \sum_i \varepsilon_i \kappa_i, \quad (3)$$

~~$$\kappa_{org} = f_{POA} * \kappa_{POA} + f_{SOA} * \kappa_{SOA}, \quad (4)$$~~

where  $\kappa_i$  and  $\varepsilon_i$  are the hygroscopicity parameter and volume fraction for the  $i$ th individual (dry) component in the mixture, respectively, and  $f_{POA}$  and  $f_{SOA}$  are the volume fractions of POA and SOA in the organic component. The AMS provides mass concentrations of organics and of many inorganic ions. The inorganic components mainly consisted of  $(\text{NH}_4)_2\text{SO}_4$  and  $\text{NH}_4\text{NO}_3$  (Zhang et al., 2014; Zhang, et al., 2016; Zhang et al., And, 2017). As noted above, the organic components mainly consisted of POA and SOA.

带格式的: 缩进: 首行缩进: 1.5 字符

带格式的: 下标

带格式的



227 ~~According to previous study~~, the values of  $\kappa$  are 0.48 for  $(\text{NH}_4)_2\text{SO}_4$  and 0.58 for  $\text{NH}_4\text{NO}_3$  (Petters and  
228 Kreidenweis, 2007). To estimate  $\kappa_{\text{org}}$ , we used the following linear function derived by Mei et al. (2013):  
229  $\kappa_{\text{org}} = 2.10 \times f_{44} - 0.11$ . We derived the volume fraction of each species by dividing mass concentration by  
230 its density. The ~~values of~~ density are ~~1720 kg m<sup>-3</sup>~~ 1.77 g cm<sup>-3</sup> for  $(\text{NH}_4)_2\text{SO}_4$  and ~~1770 kg m<sup>-3</sup>~~ 1.72 g cm<sup>-3</sup> for  
231  $\text{NH}_4\text{NO}_3$ . The densities of ~~all organics, POA, and SOA~~ are assumed to be ~~1200 kg m<sup>-3</sup>~~ 1.2 g cm<sup>-3</sup> (Turpin et  
232 al., 2001), ~~1000 kg m<sup>-3</sup>~~, and ~~1400 kg m<sup>-3</sup>~~ respectively. The  $\kappa$  and density ~~of BC of BC~~ are assumed to be 0  
233 and ~~1700 kg m<sup>-3</sup>~~ 1.7 g cm<sup>-3</sup>. In the following discussions,  $\kappa_{\text{gf}}$  and  $\kappa_{\text{chem}}$  denote the values derived from  
234 HTDMA measurements and calculated using the ZSR mixing rule, respectively.

235 In addition, we also compare the results from the field campaigns with those from other two sites,  
236 Xingtai (XT: 37.18 °N, 114.37 °E), and Xinzhou (XZ: 38.24 °N, 112.43 °E), in North China Plain (Fig. 1).  
237 At XZ site, we use the hygroscopic parameter (defined as  $\kappa_{\text{CCNc}}$ ) from size-resolved CCN measurements  
238 (Zhang et al., 2014, 2016) for comparison. More detailed descriptions of the method to retrieve  $\kappa_{\text{CCNc}}$  can be  
239 found in (Petters and Kreidenweis (2007). Both of the  $\kappa_{\text{gf}}$  and  $\kappa_{\text{CCNc}}$  are derived based on  $\kappa$ -Köhler Theory  
240 (Petters and Kreidenweis, 2007). But, different from the  $\kappa_{\text{gf}}$  measured by the HTDMA system which is  
241 operated at RH of 90%, the  $\kappa_{\text{CCNc}}$  is derived by measuring aerosols CCN activity under the condition of  
242 supersaturations with relative humidity of >100%. Previous studies from filed measurements and laboratory  
243 experiments showed that the  $\kappa_{\text{CCNc}}$  is generally slight larger or smaller than  $\kappa_{\text{gf}}$ , but they are basically  
244 comparable and can well represent an overall aerosols hygroscopicity (e.g. Carrico et al., 2008; Wex et al.,  
245 2009; Good et al., 2010; Irwin et al., 2010; Cerully et al., 2011; Wu et al., 2013; Zhang et al., 2017).

### 246 3. Results and discussion

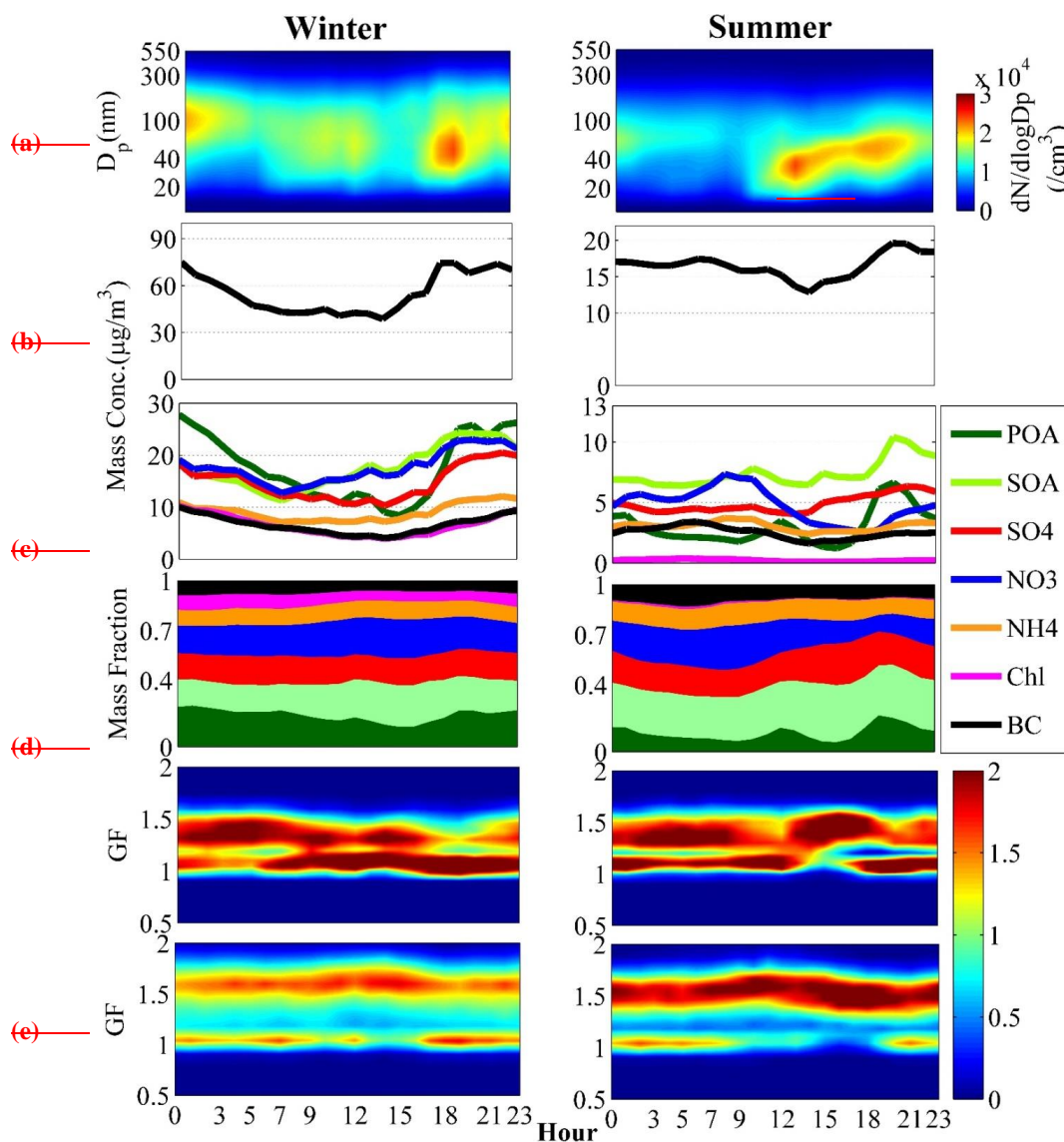
#### 247 3.1. Diurnal variations of ambient fine particles physiochemical properties and hygroscopic growth 248 factor

249 The diurnal variations of the PNSD, mass concentration of  $\text{PM}_{10}$ , mass concentration and fraction of  
250 chemical components in  $\text{PM}_{10}$ , and Gf-PDFs for 40 and 150 nm particles during the campaign are shown in

251 Fig. 3. During the summer an obvious peak value in the PNSD is observed around noontime due to NPF  
252 events that typically started around 10:00 LT (Local Time). The resulting sharp increase in number  
253 concentration of nucleation mode particles was followed by decreased concentration and a rapid growth in  
254 diameter of the particles along with increased mass concentration of SOA and sulfate in  $PM_{10}$ , indicating  
255 strong photochemical and secondary formation processes during daytime in the summer- (Marked in red box  
256 in Fig. 3). In contrast, NPF was not evident during the winter period, which may in part be due to the much  
257 higher ( $\sim 3\times$ )  $PM_{10}$  mass concentrations in the winter than in the summer.- Note that peak values in number  
258 concentration and in mass concentrations of  $PM_{10}$  and POA occurred during the early evening (17:00-21:00,  
259 LT) indicating the strong impact of local sources from traffic emissions and cooking- (Marked in black box  
260 in Fig. 3). In addition, the diurnal cycles of aerosol physical and chemical properties are also influenced by  
261 the diurnal changes in the planetary boundary layer (PBL) that leads to accumulation of particles during  
262 nighttime when higher values of both number and mass concentration were observed.

263 ~~Fig. 3e shows the diurnal variations of the Gf PDFs for 40 nm and 150 nm particles.~~ Owing to the  
264 continued local and primary emissions near the study site, the Gf-PDFs for 40 nm particles generally display  
265 a bimodal shape with more and less hygroscopic modes (with Gf of  $\sim 1.5$  and  $\sim 1.1$  respectively) throughout  
266 the day both in winter and summer periods, indicating an external mixing state for the 40 nm particles. Note  
267 that, during nighttime and early morning in the winter, the more hygroscopic mode dominated and was  
268 shifted to higher Gf than during the daytime. This is thought to be due to heterogeneous/aqueous reactions  
269 on pre-existing primary small particles, and/or coagulation/condensation processes that are enhanced at  
270 night under lower ambient temperature and higher relative humidity, all of which result in a more  
271 hygroscopic and more internally-mixed aerosol (Liu et al., 2011; Massling et al., 2005; Ye et al., 2013; Wu  
272 et al., 2016; Wang et al., 2018a). Interestingly, in the summer period, the concentration of the hydrophilic  
273 mode increased quickly around noontime and in the early afternoon (12:00-16:00), with a corresponding  
274 decrease in the relative concentration of the hydrophobic mode, which likely indicates a transformation of  
275 the particles from externally to internally mixing state as a result of the species condensation from the  
276 photochemical reaction (Wu et al., 2016; Wang et al., 2017), resulting in an increase in particle  
277 hygroscopicity ~~(Fig. S3)~~. In addition, it is evident that 40 nm particles after 12:00 were dominated by NPF

278 (Fig. 3). Therefore, the increase of hydrophobic mode particles suggests that a large amount of hydrophilic  
 279 particles are generated from NPF. For 150 nm particles, the hygroscopic mode in the Gf-PDF is more  
 280 dominant during daytime in particular during the summer period when the strong solar radiation promotes  
 281 photochemical aging and growth, thus producing a more internally-mixed aerosol. The dominant  
 282 hydrophobic mode at around 18:00 was observed both in winter and summer and reflects abundant traffic  
 283 emissions and cooking sources (primarily with POA) during the early evening period (Fig. 2e).



284

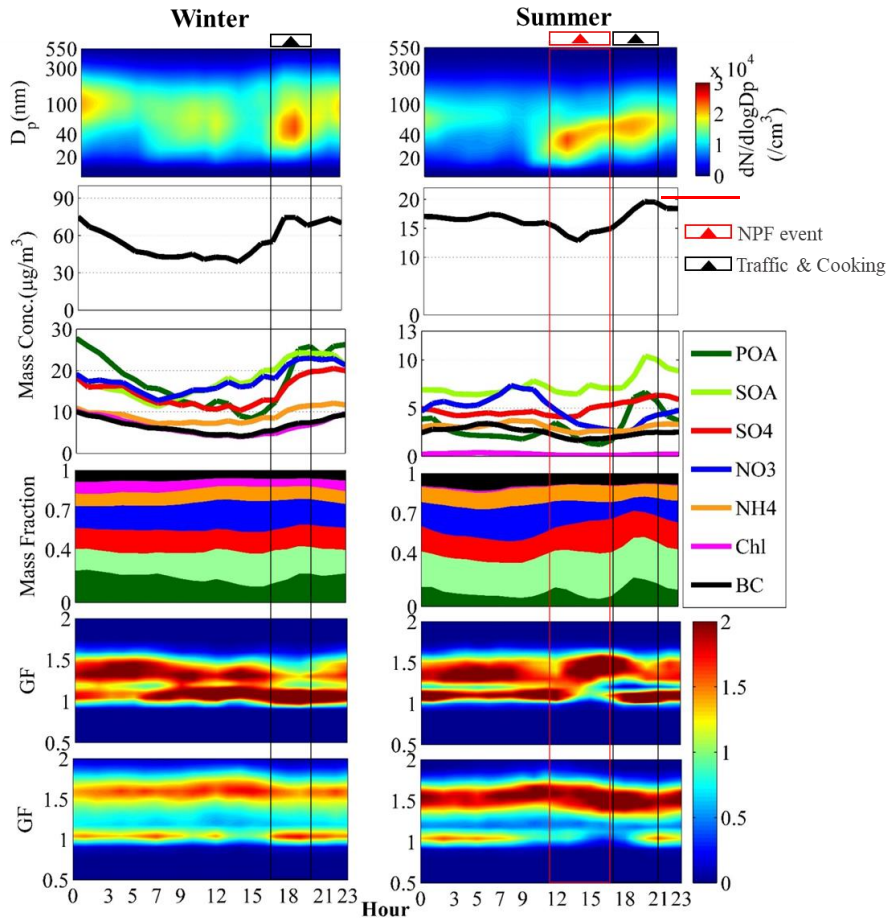
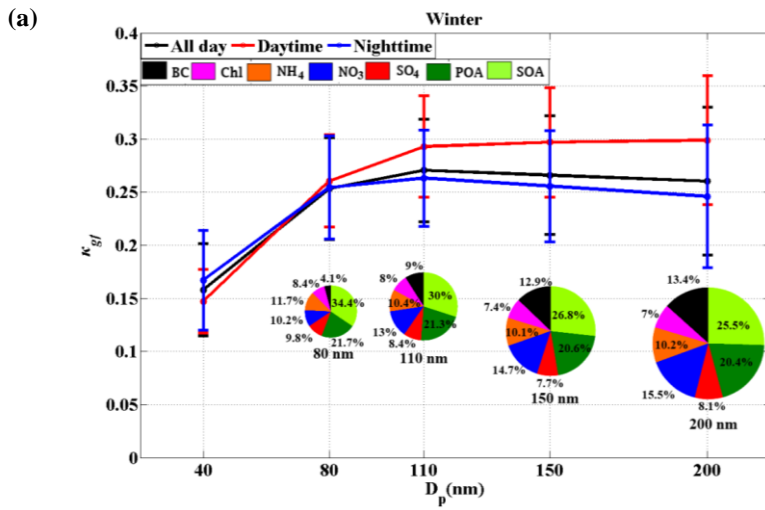


Figure 3. Diurnal Campaign averaged diurnal variations in (a) particle number size distribution; (b) mass concentration of  $PM_{10}$ ; (c) bulk mass concentration of main species in  $PM_{10}$ ; (d) mass fraction of chemical composition of  $PM_{10}$ ; (e) and Gf-PDFs for 40 and 150 nm particles in winter (left panels) and summer period (right panels) measured in urban Beijing..

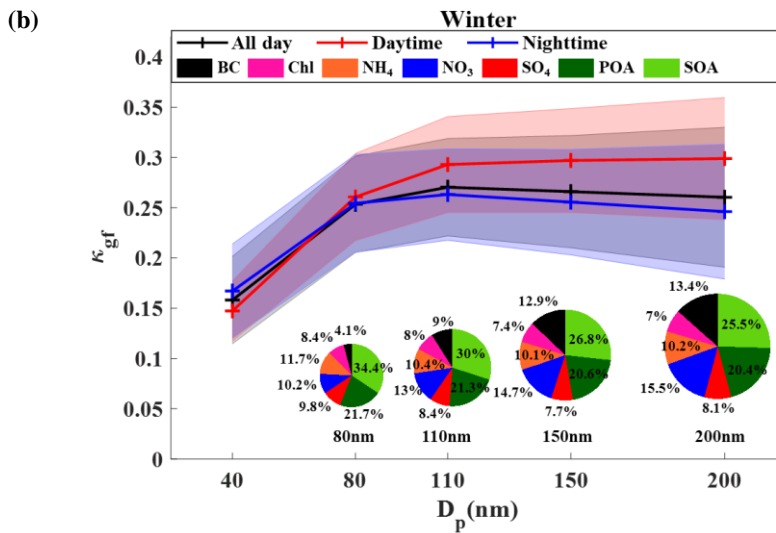
### 3.2 $\kappa_{gf}$ dependence on $D_p$

The size dependence of particle hygroscopicity parameters for the winter and summer periods are presented in Fig.4. In the winter, the 40 nm particles were least hygroscopic and the hygroscopicity of larger particles (>80 nm) displayed insignificant dependence on particle size. The size independence for the larger particles is consistent with the observed similarity in mass fractions of inorganic and organic species across

295



296



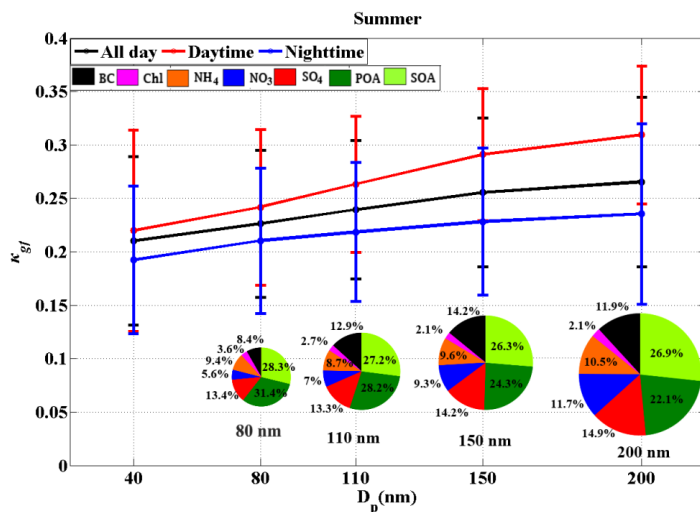
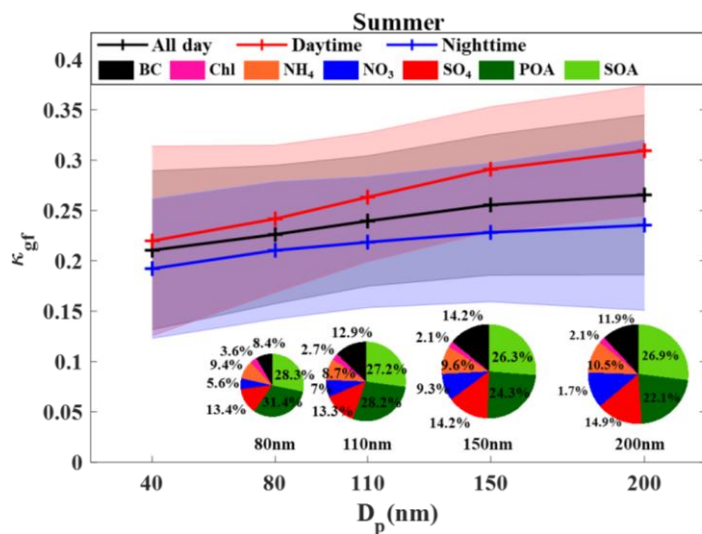


Figure 4. The dependence of  $\kappa$  on  $D_p$  at the urban Beijing site during the study periods: winter (a) and summer (b). The  $\kappa$  values are retrieved from the size-resolved HTDMA measurements. The error bars represent  $\pm 1\sigma$ . The size-resolved chemical mass fractions at the corresponding  $D_p$  is also presented.

the size range as shown in the pie charts in Figure 4a. A similar dependence of particle hygroscopicity on particle size was also observed in the urban area of Beijing during the wintertime of 2014 (Wang et al., 2018b). In the summer, hygroscopicity increased with increasing particle size, which is expected based on

the size dependent patterns shown in the pie charts, with the mass fraction of POA decreasing with the particles size and the mass fraction of inorganics like sulfate and nitrate increasing with particle size.

### 3.3. Closure of HTDMA and chemical composition derived $\kappa$

A closure study was conducted between  $\kappa_{chem}$  and  $\kappa_{gf}$  (Fig. 5) to investigate the uncertainty of the two methods, and especially to further illustrate whether particle hygroscopicity can be well predicted by  $\kappa_{chem}$  calculated by assuming internal mixing. Since a size-resolved BC mass concentration measurement was not available during the campaign, we use the bulk mass fraction of BC particles measured by the AE33 combining with size-resolved BC distribution in Beijing reported by Liu et al. (2018) to estimate  $\kappa_{chem}$ .

带格式的

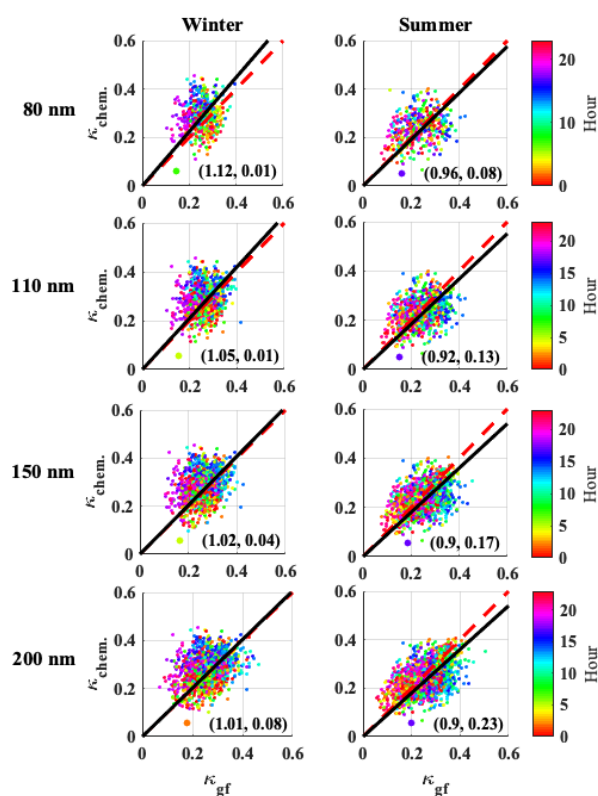


Figure 5. Closure of  $\kappa_{chem}$  calculated from size-resolved chemical composition data and  $\kappa_{gf}$  retrieved from hygroscopic growth factor by HTDMA measurements in winter (left panels) and summer (right panels) period. The dots with different color correspond to observed time of a day during the campaign as shown by

the color bar. On each plot, red dotted line is 1:1 line, black solid line is fitting line. The numbers in parentheses are slopes of linear fits and correlation coefficients ( $R^2$ ) and slopes of linear fits.

available during the campaign, we use the bulk mass fraction of BC particles measured by the AE33 combining with size-resolved BC distribution measured by a single particle soot photometer (SP2) in Beijing (Liu et al., 2018) to estimate  $\kappa_{chem}$ . During the calculation, the BC core diameter measured by SP2 has been converted to the diameter of coated BC particles by multiplying factors of 1.4 and 2.6 under clean (with bulk BC mass concentrations  $<2 \mu\text{g m}^{-3}$ ) and polluted (with bulk BC mass concentrations  $>2 \mu\text{g m}^{-3}$ ) conditions respectively (Liu et al., 2018).

Uncertainty in  $\kappa$  is due in part to measurement uncertainty of the HTDMA/CCNe system and uncertainty resulting from non-ideality effects in the solution droplets, surface tension reduction due to surface active substances, and the presence of slightly soluble substances that dissolve at RH higher than that maintained in the HTDMA (e.g., Wex et al., 2009; Good et al., 2010; Irwin et al., 2010; Cerully et al., 2011; Wu et al., 2013). However, our previous study demonstrated that, for this region, estimates using HTDMA data are still better representing the aerosols hygroscopicity than those using the simple mixing rule based on chemical volume fractions for an assumed internal mixture (Zhang et al., 2017). Therefore, here we focus on discussing and exploring the uncertainty of  $\kappa_{chem}$  by taking  $\kappa_{gf}$  as the reference.

OurThe results show that, in winter, although the slopes from linear fitting of  $\kappa_{chem}$  and  $\kappa_{gf}$  are about 0.96 close to 1.0 for particles, it is with diameters of 80, 110, 150, and 200 nm, indicating an overall consistency of  $\kappa_{chem}$  and  $\kappa_{gf}$ . In summer, the slopes are 0.88–0.89 for 110, 150, and 200 nm particles, meaning there is about 10%–12% underestimation of  $\kappa_{chem}$ . However, the quite poor correlations (typically with correlation coefficients,  $R^2$ , of  $< 0.3$ ) between  $\kappa_{chem}$  and  $\kappa_{gf}$  of the 80, 110, 150, 200 nm particles both in winter and summer. The poor correlations reflect large uncertainty in one or both of the calculated parameters. The large uncertainties that are likely due to the unreasonable assumption of particle mixing state (e.g. Cruz and Pandis, 2000; Svenningsson et al., 2006; Sjogren et al., 2007; Zardini et al., 2008), which varies with their aging and other physiochemical processes in the atmosphere. ~~For~~

带格式的: 英语(美国)

带格式的: 英语(美国)



343 ~~example, Note that~~ underestimation of  $\kappa_{chem}$  for the summer occurred mostly in the afternoon. ~~(Marked in~~  
344 ~~blue dots in Fig. 5).~~ This may be associated with photochemical processes at around noontime. More  
345 specific investigations of the particle mixing and aging impacts on  $\kappa_{chem}$  will be further addressed in the  
346 following sections.

### 347 **3.4 Atmospheric Aerosols aging processes and sources effects indicated by diurnal cycles of $\kappa_{chem}$ and**

348  $\kappa_{gf}$

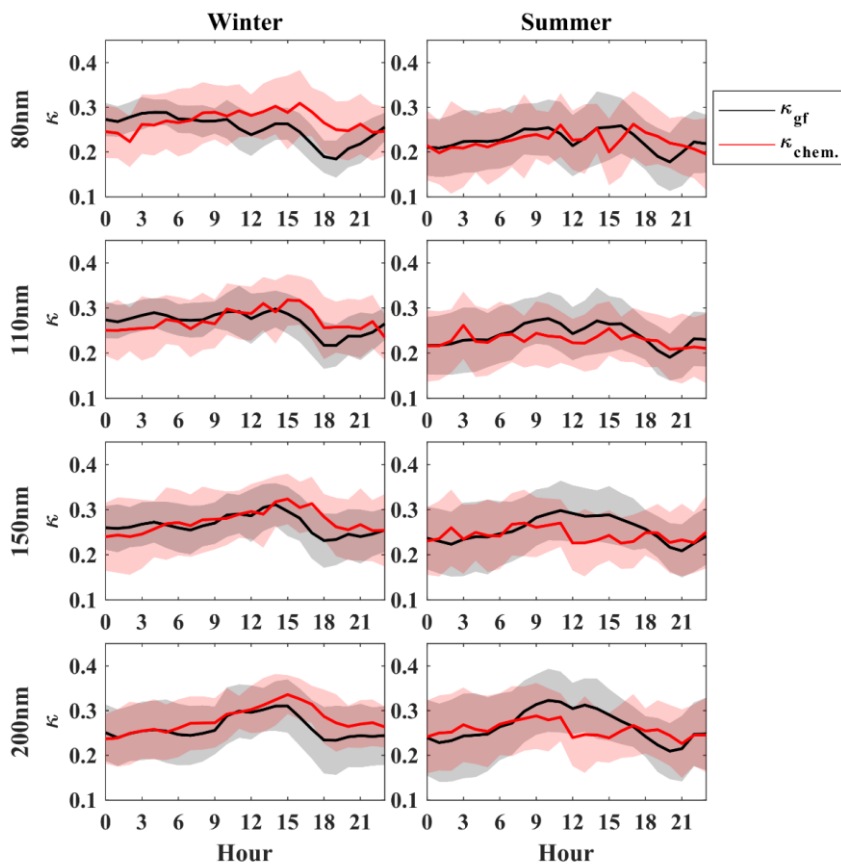
349 The diurnal cycles of particle hygroscopicity in the summer and winter with the use of the size-resolved  
350 chemical composition observations and the ratio of  $\kappa_{chem}$  to  $\kappa_{gf}$  are shown in Fig. 6. In summer, at  
351 09:00-15:00, the disparity between  $\kappa_{chem}$  and  $\kappa_{gf}$  is insignificant for smaller particles (80 and 110 nm), both  
352 of which show slight decrease from 09:00 or 10:00 to 12:00-13:00 due to the frequent NPF event that  
353 usually corresponds to a large fraction of organics (Fig. 3) in urban Beijing. For larger particles (150 and  
354 200 nm), the disparity between  $\kappa_{chem}$  and  $\kappa_{gf}$  around noontime and in the early afternoon is very significant,  
355 corresponding to >20% underestimation of particle hygroscopicity by  $\kappa_{chem}$  (with the ratio of  $\kappa_{chem}$  to  $\kappa_{gf}$  of  
356 ~0.8). Similar patterns were also noted by Zhang et al., (2017) but which is only based on a comparison  
357 between  $\kappa_{chem}$  derived from bulk chemical composition and  $\kappa_{gf}$ . Our results ~~further clarify again indicate~~ that  
358 the rapid photochemical aging of BC particles, which are generally with dominant size modes of 100-200  
359 nm in the atmosphere, ~~leads may lead~~ to the core-shell structure in which certain secondary aerosol generated  
360 from photochemical reactions is thickly coated on the surface of BC (Wang et al., 2019). The hygroscopicity  
361 of the coated BC particles may only depend on the coating layer (Ma et al., 2013), thus resulting in the  
362 noontime/early afternoon underestimation of particle hygroscopicity by  $\kappa_{chem}$ . While, no significant  
363 differences between  $\kappa_{chem}$  and  $\kappa_{gf}$  are observed during night time. Note that  $\kappa_{chem}$  is slightly higher than  $\kappa_{gf}$   
364 during early evening traffic rush hour and cooking time, when emissions of primary hydrophobic particles  
365 (e.g. BC and POA) are high (Fig. ~~3b3~~), thus resulting in a large percentage of externally-mixed particles ~~(Fig.~~  
366 ~~3e, Fig. S4 and Fig. S5). Therefore, -). Causes of the assumption of uniform internal mixing overestimation in~~  
367  ~~$\kappa_{chem}$  during the traffic rush hour and cooking time will overestimate hygroscopicity according to our~~  
368 ~~previous study (Zhang et al., 2017). But the be discussed in the following paragraph. The~~ particles

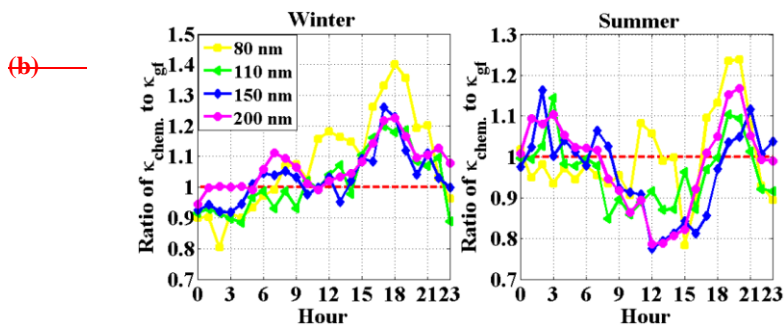
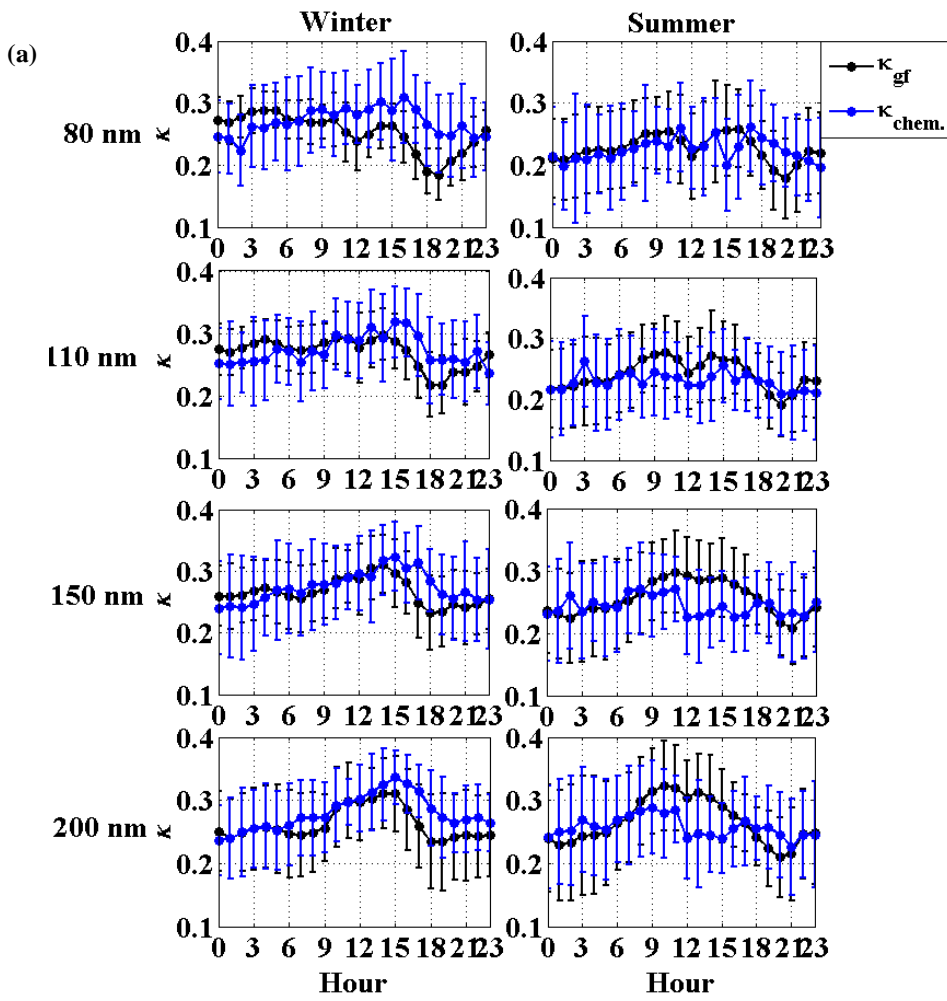
369 experience rapid conversion and mixing in urban Beijing due to high precursor gases (Sun et al., 2015; Wu  
370 et al., 2016; Ren et al., 2018), and thus the coated/aged particles produced through photochemical processing  
371 in the afternoon can mix and interact with and freshly emitted primary particles emitted during rush hour  
372 (Wu et al., 2008). Therefore, during nighttime (22:00-06:00, LT), the particles are more uniform  
373 internally-mixed, which is reflective of the assumption for calculation of  $\kappa_{chem}$ , a much better consistency  
374 between  $\kappa_{chem}$  and  $\kappa_{gf}$  is observed. ~~And due to the relatively clean conditions overall in the summer, no large~~  
375 ~~differences are observed under clean and polluted conditions (Fig. S5-S7).~~

376

377

378





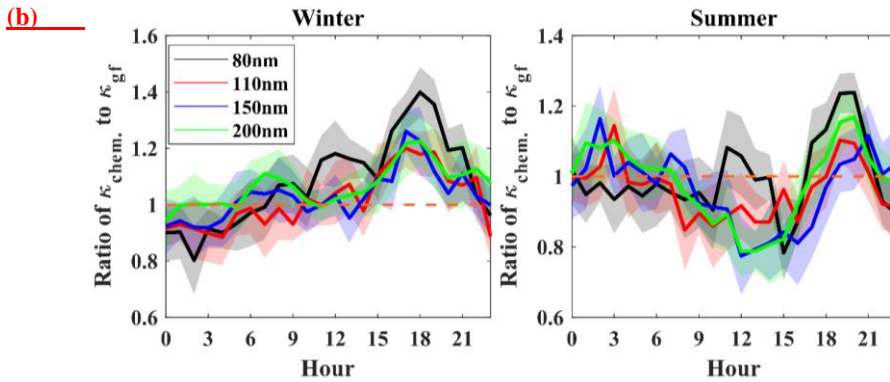
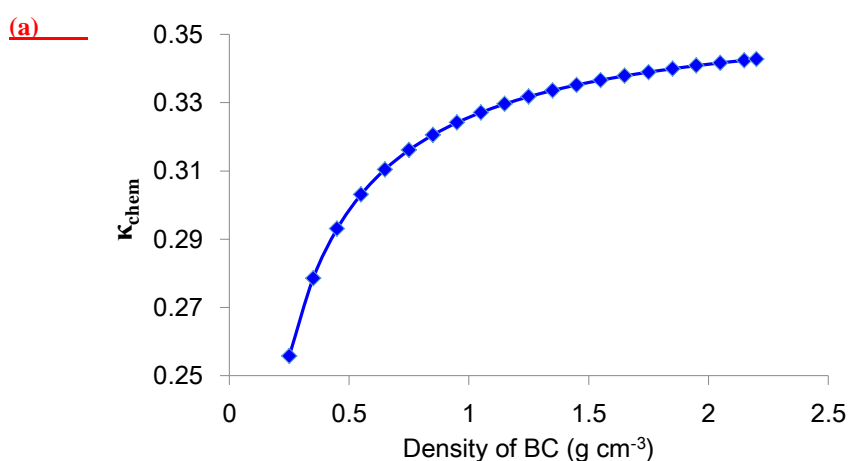


Figure 6. Diurnal variations of (a)  $\kappa_{chem}$  using size-resolved chemical composition data and  $\kappa_{gf}$  in winter and summer period; and (b) ratio of  $\kappa_{chem}$  to  $\kappa_{gf}$  in winter and summer period. The shade regions denote the error bars ( $1\sigma$ ).

In winter, the disparity between  $\kappa_{chem}$  to  $\kappa_{gf}$  is insignificant at 09:00-15:00 due to the weakening effect of photochemical aging. From 15:00 to 21:00 LT, due to the strong vehicle and cooking sources around the site, the particles are dominated by the hydrophobic mode with a large concentration of externally-mixed BC and POA particles (Fig. 3 and Fig. S8), the calculated  $\kappa_{chem}$  is much higher than  $\kappa_{gf}$ , with the maximum ratio of  $\kappa_{chem}$  to  $\kappa_{gf}$  of 1.2-1.4, and the greatest disparity is observed for small particles. The disparity is further enhanced during clean periods when the hydrophobic mode is dominant (Fig. 7, Fig. S1).

We suppose that the large disparity between  $\kappa_{chem}$  and  $\kappa_{gf}$  is due to temporal variations in actual density of BC and organics caused by the particles aging and local sources. The externally-mixed BC particles are with fractal structure and chain-like aggregates and have been reported with effective density of 0.25-0.45 g cm<sup>-3</sup> (McMurry et al., 2002). While the BC particles in the calculation is assumed as void free with effective density of 1.7 g cm<sup>-3</sup>. Such inappropriate assumption would lead to an underestimation of BC volume fraction and thus the overestimation in  $\kappa_{chem}$  during the traffic rush hour and cooking time when BC particles are mostly freshly emitted with uncompacted structure. In addition, the significant increase in volume fraction of POA during the late afternoon would result in a lower density of organics, which is expected to be smaller than the assumed one (1.2 g cm<sup>-3</sup>) in the calculation. A sensitivity test has been done to examine the effect of density of BC and organics on calculated  $\kappa_{chem}$  (Fig. 7). The result shows that the  $\kappa_{chem}$  value

402 reduces by 16-33% when applying the BC effective density of 0.25-0.45 g cm<sup>-3</sup>. This basically explains the  
403 disparity during the traffic rush hour. However, the changes in  $\kappa_{\text{chem}}$  are within  $\pm 4\%$  when changing the  
404 organic density from 1.0 (typical for POA) to 1.4 (typical for SOA) g cm<sup>-3</sup>, suggesting insensitivity of  $\kappa_{\text{chem}}$   
405 to variations of organic density. The result also indicates that, to fill the gap between  $\kappa_{\text{chem}}$  and  $\kappa_{\text{gf}}$  observed  
406 at noontime, the effective density of BC should be extremely high due to the decreased sensitivity of  $\kappa_{\text{chem}}$  to  
407 BC density with the aging of BC. In this case, the assumed density of BC is 1.7 g cm<sup>-3</sup>, which reflects a very  
408 compacted and void free structure of the BC particles. The current applied value represents an upper limit  
409 for the effective density of ambient BC particles according to previous observations at a site near urban  
410 Beijing (Zhang et al., 2015), which suggested the aged BC is generally with effective density of 1.2 g cm<sup>-3</sup>.  
411 Using this ambient observed density would lead to further underestimation in  $\kappa_{\text{chem}}$ . Our results exhibit the  
412 increase of the density of BC and organics cannot explain the disparity between  $\kappa_{\text{chem}}$  and  $\kappa_{\text{gf}}$  observed  
413 around noontime in summer. This just, on the other hand, verifies the photochemical aging/coating effect on  
414 the aerosols hygroscopicity. In addition, the coexisting hygroscopic and hydrophobic species may have a  
415 strong influence on the phase state of particles, also likely affecting chemical interactions between inorganic  
416 and organic compounds as well as the overall hygroscopicity of mixed particles (Peng et al., 2016). Further  
417 investigations are needed to verify this. Our study suggest that, to accurately parameterize the effect of BC  
418 aging on particles hygroscopicity, future investigations need to measure the effective density and morphology  
419 of ambient BC, in particularity in those regions with complex local sources.



(b)

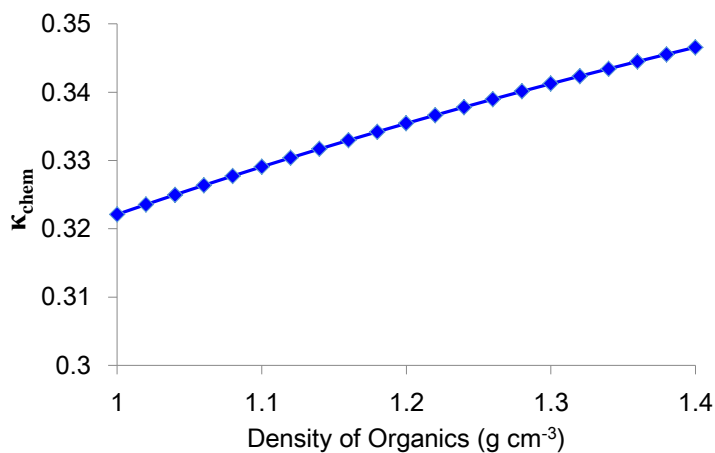


Figure 8. Sensitivity of  $\kappa_{chem}$  to variations of density of BC (a) and organics (b)

Besides the impacts of BC aging (changes in morphology/density) and variations of the overall density of organics on particles hygroscopicity, uncertainty in  $\kappa_{chem}$  may be related to the uncertainty in the hygroscopic parameter for organics that could vary widely over a range of diverse constituents of SOA (Suda et al., 2012). However, Zhang et al. (2017) shown that using a smaller or larger  $\kappa_{SOA}$  could not fully explain the overestimation during traffic hours or the underestimation around noontime. Furthermore, in this study, it is calculated from a simple parametrized equation based on the AMS-measured  $f_{44}$  value reported by Mei et al. (2013). The value for  $f_{44}$  tends to be overestimated according to Fröhlich et al. (2015), which should yield a larger  $\kappa_{chem}$ . Previous studies have shown that freshly emitted POA and BC particles may be rapidly coated by more hygroscopic components in polluted urban areas, resulting in enhanced hygroscopicity of the mixed particles (Zhang et al., 2004; Johnson et al., 2005; Zhao et al., 2017). Our results are consistent with those observations and clarify the photochemical aging and coating effect will largely underestimate the particles hygroscopicity using simple mixing rule based on chemical composition.

Note that during the nighttime,  $\kappa_{chem}$  is slight lower than  $\kappa_{gf}$  with the minimum ratio of  $\kappa_{chem}$  to  $\kappa_{gf}$  of ~0.8 for 80 nm particles and ~0.9 for 110 and 150 nm particles at 02:00-04:00 LT (Fig. 6b), indicating an underestimation of particle hygroscopicity using composition data. The disparity at nighttime is further increased during heavily polluted events (Fig. S1), when the particles are more internally-mixed with only



one hygroscopic mode (Fig. 8). We propose the increased underestimation during polluted conditions is likely due to enhanced condensation of secondary hygroscopic compounds (e.g. nitrate, sulfate) on pre-existing aerosols at lower temperature and higher relative humidity at nighttime (Wu et al., 2008; Wang et al., 2016; An et al., 2019). However, such condensation effect during nighttime is less significant (indicated by the smaller disparity between  $\kappa_{chem}$  and  $\kappa_{gf}$ ) than the coating effect caused by aerosols photochemical aging at noontime, likely due to thinner coating layer formed on the pre-exist particles during nighttime or other factors influencing the particles hygroscopicity.

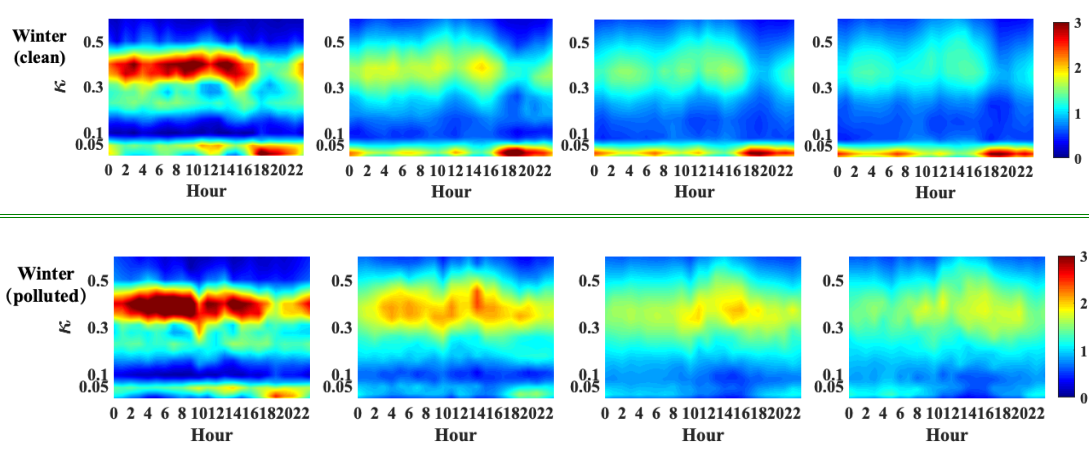


Figure 8. Diurnal cycles of  $\kappa_{gf}$ -PDF for 80, 110, 150 and 200 nm particles in clean and polluted events in winter.

### 3.5. Observation from other stations

The aging process in the summer period is related to photochemical processing in strong solar radiation conditions. The photochemical reactions produce sulfate and secondary organic aerosol, condensing on the surface of slightly- or non-hygroscopic primary aerosols (such as BC) (Zhang et al., 2008). As discussed in 3.4, the core-shell structure that accompanies aging of the particles results in calculated  $\kappa_{chem}$  that underestimates their hygroscopicity. To confirm such a coating effect on particle hygroscopicity, we further

examine the diurnal variations of  $\kappa_{chem}$  and  $\kappa_{gf}$  or  $\kappa_{CCNC}$ .

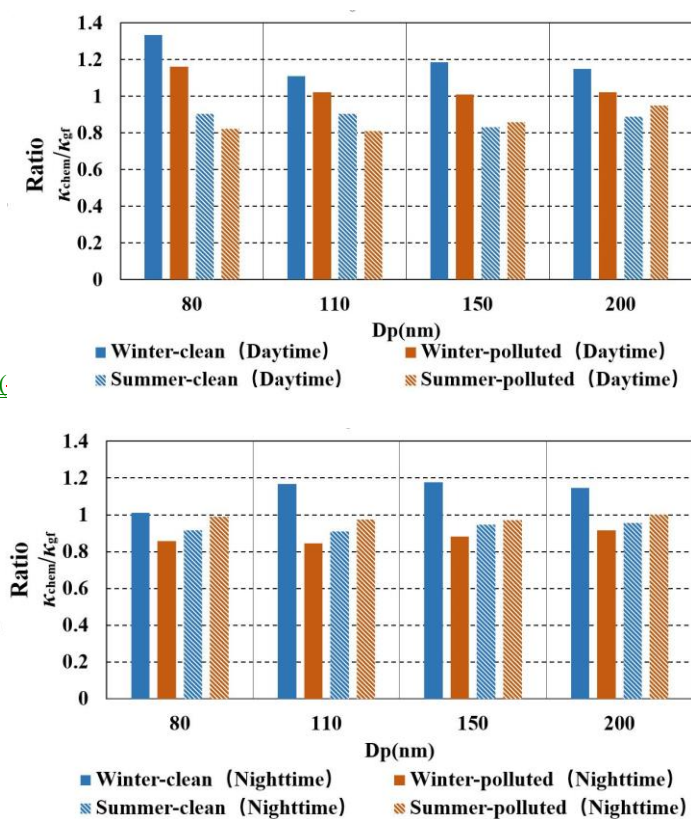


Figure 7. Ratio of mean  $\kappa_{chem}$  to  $\kappa_{gf}$  during daytime (top panel) and nighttime (bottom panel) under clean/polluted conditions between winter and summer period.

disparity is further enhanced during clean periods (Fig. S7, Fig. S9 and Fig. 7) when the hydrophobic mode is dominant (Fig. 8). But note that during the nighttime,  $\kappa_{chem}$  is slight lower than  $\kappa_{gf}$ , with the minimum ratio of  $\kappa_{chem}$  to  $\kappa_{gf}$  of 0.8 for 80 nm particles and 0.9 for 110 and 150 nm particles at 02:00–04:00 LT (Fig. 6b), indicating an underestimation of particle hygroscopicity using composition data. The disparity at nighttime is further increased during heavily polluted events (Fig. 7 and Fig. S9), when the particles are more internally mixed with only one hygroscopic mode (Fig. 8 and Fig. S8). We believe the increased underestimation during polluted conditions is likely due to enhanced condensation of secondary hygroscopic compounds (e.g. nitrate, sulfate) on pre-existing aerosols at lower temperature and higher relative humidity at nighttime (Wu et al., 2008; Wang et al., 2016; An et al., 2019).

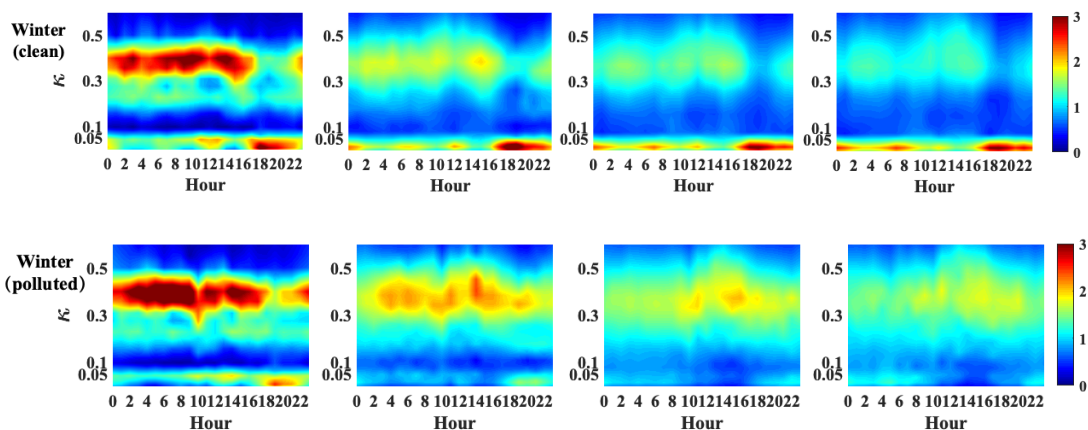


Figure 8. Diurnal cycles of  $\kappa_{gf}$  - PDF for 80, 110, 150 and 200 nm particles in clean and polluted events in winter.

### 3.5. Observation from other stations

The aging process in the summer period is related to photochemical processing in strong solar radiation conditions. The photochemical reactions produce sulfate and secondary organic aerosol, condensing on the surface of slightly or non-hygroscopic primary aerosols (such as black carbon) (Zhang et al., 2008). As discussed in 3.4, the core-shell structure that accompanies aging of the particles results in calculated  $\kappa_{chem}$  that underestimates their hygroscopicity. To confirm such a coating effect on particle hygroscopicity, we further examine the diurnal variations of  $\kappa_{chem}$  and  $\kappa_{gf}$  or  $\kappa_{CCN}$  (derived from CCN measurements only at XZ site) based on observations in summer at two other sites in north China (Fig. 1). The XT site is located in the suburb of XT city, which is about 400 km south of Beijing, with high levels of industrialization and urbanization. Due to industrial emissions and typically weak ventilating winds, concentrations of  $PM_{2.5}$ , black carbon and gaseous precursors are usually high at the site (Fu et al., 2014). Xinzhou is located in north of Taiyuan and about 360 km southwest of Beijing, and is surrounded by mountains on three sides. Local emissions from motor vehicles and industrial activities have relatively little influence on the sampled aerosol (Zhang et al., 2016). We Because of its location and elevation, the aerosol at the XZ site is usually aged and transported from other areas. The sampling period was from July 22 to August 26, 2014 and from May 17 to June 14, 2016 at XZ and XT site respectively.

491 We find that the case at the Xingtai (XT) site is very similar to that observed in Beijing (BJ (Fig. 9a),  
492 with a lower  $\kappa_{chem}$  than  $\kappa_{gf}$  around noon time. But, because of much less influences from the local sources at  
493 XT compared to that at BJ, such underestimation by  $\kappa_{chem}$  continued until night at XT (Fig. 9b). Interestingly,  
494 a noontime lower  $\kappa_{chem}$  was not observed in the diurnal cycles at the ~~But, because of much less influences~~  
495 ~~from the local sources at XT compared to that at BJ, such underestimation by  $\kappa_{chem}$  continued until night at~~  
496 ~~XT (Fig. 9b). Interestingly, a noontime lower  $\kappa_{chem}$  was not observed in the diurnal cycles at the Xinzhou~~  
497 ~~(XZ) site, where  $\kappa_{chem}$  and  $\kappa_{CCNc}$  had similar diurnal patterns (Fig. 9c) with a roughly constant ratio of  $\kappa_{chem}$  to~~  
498  $\kappa_{CCNc}$  of ~0.8-0.9- (Fig. 9d). This is probably because the XZ site is usually the recipient of aerosols  
499 transported from other areas that are already aged and well-mixed, with minimal impact of additional  
500 coating (Zhang et al., 2017). Also, the rate of oxidation and condensation may be slow in the relatively  
501 remote area where the gas precursors and oxidants are not as high as they are closer to sources regions. But  
502 at XT, which is located in the heavily polluted area in the north China Plain (Fu et al., 2014), aerosol  
503 emissions and processing are more similar to that in urban Beijing. These observations from other sites  
504 further confirms the the photochemical aging and coating effect that will largely underestimate the particles  
505 hygroscopicity using simple mixing rule based on chemical composition.

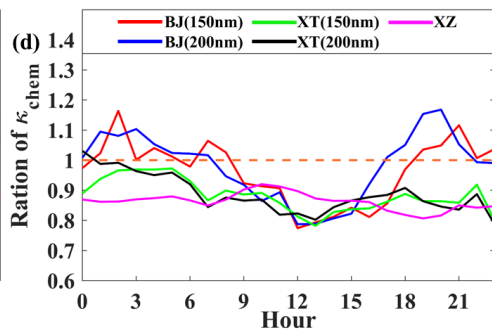
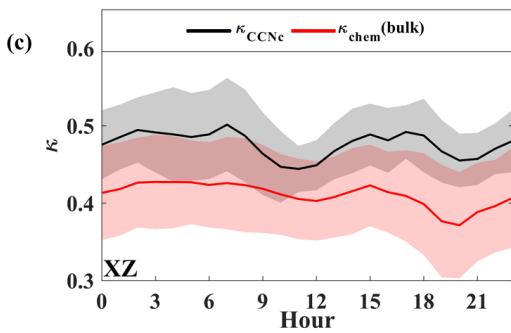
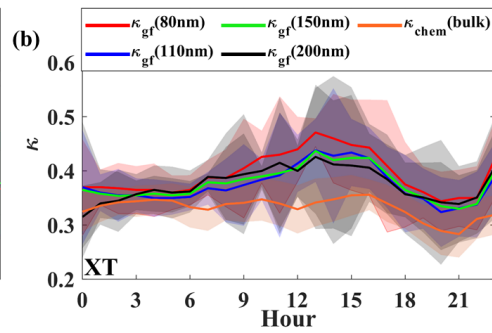
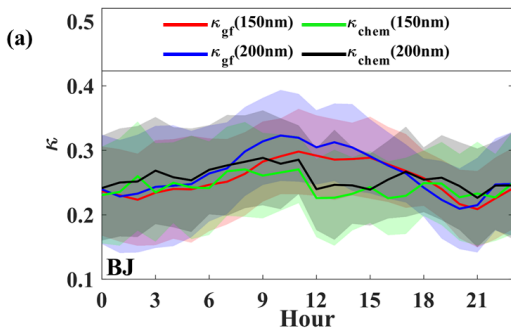
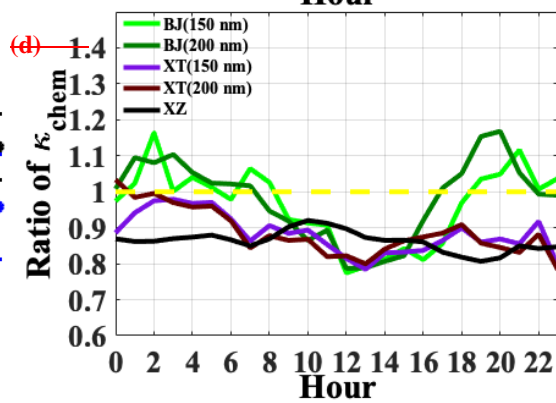
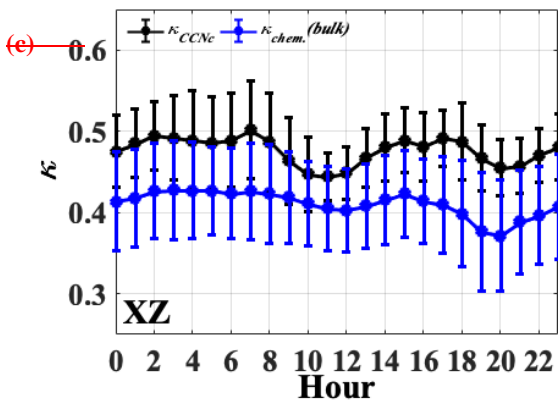
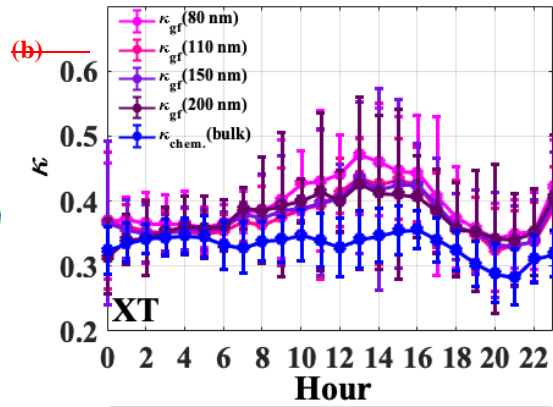
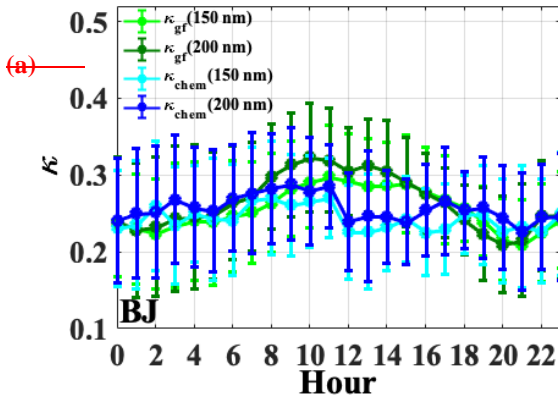


Figure 9. Diurnal variations in (a)  $\kappa_{chem}$  and  $\kappa_{gf}$  for 150 and 200 nm particles at BJ site; (b)  $\kappa_{chem}$  and  $\kappa_{gf}$  for 40, 80, 110, 150 and 200 nm particles at XT site; (c)  $\kappa_{chem}$  and mean  $\kappa_{CCNc}$  for particles at XZ site, and (d) ratio of mean  $\kappa_{chem}$  to  $\kappa_{gf}$  at the three sites.

~~Although the underestimation in  $\kappa_{chem}$  may be also related to the uncertainty in the hygroscopic parameter for organics, which is calculated from a simple parametrized equation based on the AMS measured  $f_{44}$  value reported by Mei et al. (2013), Zhang et al. (2017) has shown that even the large underestimation of  $\kappa_{SO_4}$  could not fully explain that of  $\kappa_{chem}$ . Furthermore, the value for  $f_{44}$  tends to be overestimated according to Fröhlich et al. (2015), which should lead to a larger  $\kappa_{chem}$ . Previous studies have shown that freshly emitted POA and BC particles may be rapidly coated by more hygroscopic components in polluted urban areas, resulting in enhanced hygroscopicity of the mixed particles (Zhang et al., 2004; Johnson et al., 2005; Zhao et al., 2017). Our results are consistent with those observations and clarify the photochemical aging and coating effect will largely underestimate the particles hygroscopicity using simple mixing rule based on chemical composition.~~

#### 4. Conclusion

Using measurements of aerosol composition and hygroscopicity made in Beijing (BJ) during a winter period of 2016 and a summer period of 2017, this paper analyzes the daily variation and seasonal differences of size-resolved aerosol hygroscopicity in urban Beijing. We mainly focus on studying the disparity of  $\kappa_{gf}$  and  $\kappa_{chem}$  between summer and winter to reveal the impact of atmospheric processes and mixing state of the particles on its hygroscopicity. The uncertainty in calculating  $\kappa$  by using chemical composition with a uniform internal mixing hypothesis is elucidated from the diurnal variations of the difference between the calculated values: in summer, lower  $\kappa_{chem}$  is obtained around noontime, with a ratio of  $\kappa_{chem}$  to  $\kappa_{gf}$  of about 0.8-0.9 for large particles (i.e. 150 nm and 200 nm), showing an underestimation of particles hygroscopicity by using simple mixing rule based on chemical composition. Combining with the observation from [XingtaiXT](#) and [XinzhouXZ](#), we attribute the underestimation to the rapid noontime photochemical aging processes in summer, which induces the coating effect that will lead to a lower  $\kappa$  if assuming a uniform mixing of the particles. In contrast, larger  $\kappa_{chem}$  than  $\kappa_{gf}$  for >100 nm particles around noontime and in the

534 early afternoon is derived in winter, with the maximum ratio of  $\kappa_{chem}$  to  $\kappa_{gf}$  of 1.2-1.4 when the particles are  
535 dominated by the hydrophobic mode with a large number of externally-mixed POA particles from strong  
536 vehicle and cooking sources. ~~We suggest that, by using the simple mixing rule, the particles hygroscopicity  
537 can be underestimated up to 10% 20% for aged aerosols due to the coating effect, but will be maximally  
538 overestimated 20 40% for externally mixed particles. We attribute this large disparity between  $\kappa_{chem}$  and  $\kappa_{gf}$   
539 to changes of BC morphology that can be indicated by effective density of BC. The sensitivity test shows  
540 that it can well explain the disparity during the traffic rush hour by applying BC effective density of  
541 0.25-0.45 g cm<sup>-3</sup>. However, we suggest that,  
542 to accurately parameterize or account for the effect of BC density on particles hygroscopicity, future  
543 investigations need to measure the effective density of ambient BC, in particularity in those regions with  
544 complex local sources.~~

545 A lower  $\kappa_{chem}$  than  $\kappa_{gf}$  for 80, 110 and 150 nm particles during the nighttime of winter is also noted, and  
546 the disparity is further enlarged in polluted days, probably due to a nighttime coating effect driven by  
547 condensation of secondary hygroscopic species on pre-existing aerosols in cold season. Our results highlight  
548 the impacts of atmospheric processes, sources on aerosol mixing state and hygroscopicity, which should be  
549 quantified and considered in models for different atmospheric conditions. ~~Long term observations from  
550 more ground sites, as well as experiments in smog chambers, should be made to parameterize such impact in  
551 model simulations.~~

552  
553 *Data availability.* All data needed to evaluate the conclusions in the paper are present in the paper and/or the  
554 Supplementary Materials. Also, all data used in the study are available from the corresponding author upon  
555 request (fang.zhang@bnu.edu.cn).

556 *Author contributions.* F.Z. and ~~X.F.J.L~~ conceived the conceptual development of the manuscript. X. F.  
557 directed and performed of the experiments with L.C., X.J., Y. W., and F. Z.. ~~X.F.Z., J.L.,~~ and ~~X.F.Z.~~  
558 conducted the data analysis and wrote the draft of the manuscript, and all authors edited and commented on  
559 the various sections of the manuscript. J.L. and X.F. contribute equally to this work.

560 *Competing interests.* The authors declare no competing interests.

561 | *Acknowledgements.* This work was funded by ~~the National Key R&D Program of China (grant no.~~  
562 | ~~2017YFC1501702),~~ National Natural Science Foundation of China (NSFC) research projects (grant nos.  
563 | ~~41975174, 41675141, 91544217),~~ the National Key R&D Program of China (grant no. 2017YFC1501702).

564 | We thank all participants of the field campaign for their tireless work and cooperation.

## 565 | **References**

566 | An, Z., Huang, R. J., Zhang, R., Tie, X., Li, G., Cao, J., Zhou, W., Shi, Z., Han, Y., Gu, Z., ~~&~~ Ji, Y.:  
567 | Severe haze in Northern China: A synergy of anthropogenic emissions and atmospheric processes,  
568 | Proceedings of the National Academy of Sciences, 116(18), 8657-8666, doi:10.1073/pnas.1900125116,  
569 | 2019.

570 | Bougiatioti, A., Fountoukis, C., Kalivitis, N., Pandis, S. N., Nenes, A., ~~&~~ Mihalopoulos, N.: Cloud  
571 | condensation nuclei measurements in the marine boundary layer of the Eastern Mediterranean: CCN  
572 | closure and droplet growth kinetics, Atmos. Chem. Phys., 9, 7053–7066, doi: 10.5194/acp-9-7053-2009,  
573 | 2009.

574 | ~~Carrico, C. M., M. D. Petters, S. M. Kreidenweis, J. L. Collett Jr., G. Engling, and Malm W. C.: Aerosol~~  
575 | ~~hygroscopicity and cloud droplet activation of extracts of filters from biomass burning experiments, J.~~  
576 | ~~Geophys. Res., 113, D08206, doi:10.1029/2007JD009274, 2008.~~

577 | Cerully, K. M., Raatikainen, T., Lance, S., Tkacik, D., Tiitta, P., Petäjä T., Nenes, A. : Aerosol  
578 | hygroscopicity and CCN activation kinetics in a boreal forest environment during the 2007 EUCAARI  
579 | campaign, Atmos. Chem. Phys., 11, 12369–12386, doi: 10.5194/acp-11-12369-2011, 2011.

580 | Chang, R.-W., Liu, P., Leaitch, W., and Abbatt, J.: Comparison between measured and predicted CCN  
581 | concentrations at Egbert, Ontario: Focus on the organic aerosol fraction at a semi-rural site, Atmos.  
582 | Environ., 41, 8172–8182, 2007.

583 | ~~Chen, C., Fan, X., Shaltout, T., Qiu, C., Ma, Y., Goldman, A., and Khalizov, A. F.: An unexpected~~  
584 | ~~restructuring of combustion soot aggregates by sub-nanometer coatings of polycyclic aromatic~~  
585 | ~~hydrocarbons, Geophys. Res. Lett., 43, 11080–11088, 2016.~~



586 Collins, D. R., Flagan, R. C., and Seinfeld, J. H.: Improved inversion of scanning DMA data, *Aerosol Sci.*  
587 *Technol.*, 36(1), 1–9, 2002.

588 Cruz, C. N. and Pandis, S. N.: Deliquescence and hygroscopic growth of mixed inorganic-organic  
589 atmospheric aerosol, *Environ. Sci. Technol.*, 34, 4313–4319, doi: 10.1021/es9907109, 2000.

590 DeCarlo, P. F., Kimmel, J. R., Trimborn, A., Northway, M. J., Jayne, J. T., Aiken, A. C., Gonin, M., Fuhrer,  
591 K., Horvath, T., Docherty, K., Worsnop, D. R., and Jimenez, J. L.: Field-deployable, high-resolution,  
592 time-of-flight aerosol mass spectrometer, *Anal. Chem.*, 78, 8281–8289, doi: 10.1021/ac061249n, 2006.

593 Fors, E. O., Swietlicki, E., Svenningsson, B., Kristensson, A., Frank, G. P., and Sporre, M.: Hygroscopic  
594 properties of the ambient aerosol in southern Sweden – a two year study, *Atmos. Chem. Phys.*, 11, 8343–  
595 8361, doi: 10.5194/acp-11-8343-2011, 2011.

596 Fröhlich, R., Crenn, V., Setyan, A., Belis, C. A., Canonaco, F., Favez, O., Riffault, V., Slowik, J. G.,  
597 Aas, W., Aizola, M., Alastuey, A., Artíñano, B., Bonnaire, N., Bozzetti, C., Bressi, M., Carbone, C., Coz,  
598 E., Croteau, P. L., Cubison, M. J., Esser-Gietl, J. K., Green, D. C., Gros, V., Heikkinen, L., Herrmann, H.,  
599 Jayne, J. T., Lunder, C. R., Minguillón, M. C., Mocnik, G., O’Dowd, C. D., Ovadnevaite, J., Petralia, E.,  
600 Poulain, L., Priestman, M., Ripoll, A., Sarda-Estève, R., Wiedensohler, A., Baltensperger, U., Sciare, J.,  
601 and Prévôt, A. S. H.: ACTRIS ACSM intercomparison – Part 2: Intercomparison of ME-2 organic source  
602 apportionment results from 15 individual, co-located aerosol mass spectrometers, *Atmos. Meas. Tech.*, 8,  
603 2555–2576, doi:10.5194/amt-8-2555-2015, 2015.

604 Fu, G. Q., Xu, W. Y., Yang, R. F., Li, J. B., & Zhao, C. S.: The distribution and trends of fog and haze in  
605 the North China Plain over the past 30 years, *Atmos. Chem. Phys.*, 14, 11949–11958, doi:  
606 10.5194/acp-14-11949-2014, 2014.

607 Gasparini, R., R. Li, and D. R. Collins: Integration of size distributions and size-resolved hygroscopicity  
608 measured during the Houston Supersite for compositional categorization of the aerosol, *Atmos. Environ.*,  
609 38, 3285–3303, doi:10.1016/j.atmosenv.2004.03.019, 2004.

610 Good, N., Topping, D. O., Allan, J. D., Flynn, M., Fuentes, E., Irwin, M., Williams, P. I., Coe, H., and  
611 McFiggans, G.: Consistency between parameterisations of aerosol hygroscopicity and CCN activity

612 during the RHaMBLe discovery cruise, *Atmos. Chem. Phys.*, 10, 3189–3203, doi:  
613 10.5194/acp-10-3189-2010, 2010.

614 Gunthe, S. S., King, S. M., Rose, D., Chen, Q., Roldin, P., Farmer, D. K., Jimenez, J. L., Artaxo, P., Andreae,  
615 M. O., Martin, S.T., and Pöschl, U.: Cloud condensation nuclei in pristine tropical rainforest air of  
616 Amazonia: size-resolved measurements and modeling of atmospheric aerosol composition and CCN  
617 activity, *Atmos. Chem. Phys.*, 9, 7551–7575, doi: 10.5194/acp-9-7551-2009, 2009.

618 Gysel, M., Crosier, J., Topping, D. O., Whitehead, J. D., Bower, K.N., Cubison, M. J., Williams, P. I., Flynn,  
619 M. J., McFiggans, G.B., and Coe, H.: Closure study between chemical composition and hygroscopic  
620 growth of aerosol particles during TORCH2, *Atmos. Chem. Phys.*, 7, 6131–6144, doi:  
621 10.5194/acp-7-6131-2007, 2007.

622 Gysel, M., McFiggans, G. B., and Coe, H.: Inversion of tandem differential mobility analyser (TDMA)  
623 measurements, *J. Aerosol Sci.*, 40, 134–151, doi: 10.1016/j.jaerosci.2008.07.013, 2009.

624 Hu, W., Hu, M., Hu, W., Jimenez, J. L., Yuan, B., Chen, W., Wang, M., Wu, Y., Chen, C., Wang, Z., Peng,  
625 J., Zeng, L., and Shao, M.: Chemical composition, sources, and aging process of submicron aerosols in  
626 Beijing: Contrast between summer and winter, *J. Geophys. Res.*, 121, 1955–1977, doi:  
627 10.1002/2015JD024020, 2016.

628 Irwin, M., Good, N., Crosier, J., Choularton, T. W., & McFiggans, G.: Reconciliation of measurements of  
629 hygroscopic growth and critical supersaturation of aerosol particles in central Germany *Atmos. Chem.*  
630 *Phys.*, 10, 11737–11752, doi:10.5194/acp-10-11737-2010, 2010.

631 Jacobson, M.Z. : Strong radiative heating due to the mixing state of black carbon in atmospheric aerosols,  
632 *Nature*, 409(6821):695-697, 2001.

633 Johnson, K. S., Zuberi, B., Molina, L. T., Molina, M. J., Iedema, M. J., Cowin, J. P., Gaspar, D. J., Wang, C.,  
634 and Laskin, A.: Processing of soot in an urban environment: Case study from the Mexico City  
635 Metropolitan Area, *Atmos. Chem. Phys.*, 5, 3033–3043, doi: 10.5194/acp-5-3033-2005, 2005.

636 Kulmala, M., Petaja, T., Monkkonen, P., Koponen, I.K., Dal Maso, M., Aalto, P.P., Lehtinen, K.E.J., and  
637 Kerminen, V.M. : On the growth of nucleation mode particles: source rates of condensable vapor in  
638 polluted and clean environments, *Atmos. Chem. Phys.*, 5, 409–416, doi: 10.5194/acp-5-409-2005, 2005.

639 Kuwata, M., Kondo, Y., Miyazaki, Y., Komazaki, Y., Kim, J. H., Yum, S. S., Tanimoto, H., and Matsuedda,  
640 H.: Cloud condensation nuclei activity at Jeju Island, Korea in spring 2005, *Atmos. Chem. Phys.*, 8,  
641 2933–2948, doi:10.5194/acp-8-2933-2008, 2008.

642 ~~Lee, A. K. Y., Willis, M. D., Healy, R. M., Onasch, T. B., and Abbatt, J. P. D.: Mixing state of carbonaceous~~  
643 ~~aerosol in an urban environment: single particle characterization using the soot particle aerosol mass~~  
644 ~~spectrometer (SP-AMS), *Atmos. Chem. Phys.*, 15, 1823–1841, doi: 10.5194/acp-15-1823-2015, 2015.~~

带格式的: 图案: 清除 (白色)

645 Liu, D., Joshi, R., Wang, J., Yu, C., Allan, J. D., Coe, H., Flynn, M. J., Xie, C., Lee, J., Squires, F., Kotthaus,  
646 S., Grimmond, S., Ge, X., Sun, Y., and Fu, P.: Contrasting physical properties of black carbon in urban  
647 Beijing between winter and summer, *Atmos. Chem. Phys. Discuss.*, doi: 10.5194/acp-2018-1142, in  
648 review, 2018.

649 Liu, P. F., Zhao, C. S., Göbel, T., Hallbauer, E., Nowak, A., Ran, L., Xu, W. Y., Deng, Z. Z., Ma, N.,  
650 Mildner, K., Henning, S., Stratmann, F., and Wiedensohler, A.: Hygroscopic properties of aerosol  
651 particles at high relative humidity and their diurnal variations in the North China Plain, *Atmos. Chem.*  
652 *Phys.*, 3479–3494, doi:10.5194/acp-11-3479-2011, 2011.

653 Ma, Y., Brooks, S. D., Vidaurre, G., Khalizov, A. F., Wang, L., and Zhang, R.: Rapid modification of  
654 cloud-nucleating ability of aerosols by biogenic emissions, *Geophys. Res. Lett.*, 40, 6293–6297, doi:  
655 10.1002/2013GL057895, 2013.

656 Massling, A., Stock, M., and Wiedensohler, A.: Diurnal, weekly, and seasonal variation of hygroscopic  
657 properties of submicrometer urban aerosol particles, *Atmos. Environ.*, 39(21), 3911–3922, doi:  
658 10.1016/j.atmosenv.2005.03.020, 2005.

659 McMurry, P. H.; Wang, X.; Park, K.; Ehara, K. The Relationship between Mass and Mobility for  
660 Atmospheric Particles. *Aerosol Sci. Technol.*, 36, 227-238, 2002.

661 Mei, F., Hayes, P. L., Ortega, A. M., Taylor, J. W., Allan, J. D., Gilman, J. B., Kuster, W. C., de Gouw, J. A.,  
662 Jimenez, J. L., and Wang, J.: Droplet activation properties of organic aerosols observed at an urban site  
663 during CalNex-LA, *J. Geophys. Res.*, 118, 2903–2917, doi: 10.1002/jgrd.50285, 2013.

664 Mikhailov, E. F., Mironov, G. N., Pöhlker, C., Chi, X., Krüger, M. L., Shiraiwa, M., Förster, J. D., Pöschl,  
665 U., Vlasenko, S. S., Ryshkevich, T. I., Weigand, M., Kilcoyne, A. L. D., and Andreae, M. O.: Chemical

666 composition, microstructure, and hygroscopic properties of aerosol particles at the Zotino Tall Tower  
667 Observatory (ZOTTO), Siberia, during a summer campaign, *Atmos. Chem. Phys.*, 15, 8847–8869,  
668 doi:10.5194/acp-15-8847-2015, 2015.

669 [Peng, C., Jing, B., Guo, Y. C., Zhang, Y. H., and Ge, M. F.: Hygroscopic behavior of multicomponent  
670 aerosols involving nacl and dicarboxylic acids. \*J. Phys. Chem. A\*, 120\(7\), 1029-1038, 2016.](#)

671 [Peng, J., Hu, M., Guo, S., Du, Z., Shang, D., and Zheng, J.: Ageing and hygroscopicity variation of black  
672 carbon particles in beijing measured by a quasi-atmospheric aerosol evolution study \(quality\) chamber.  
673 \*Atmospheric Chemistry and Physics\*, 17\(17\), 10333-10348, 2017.](#)

674 Petters, M. D. and Kreidenweis, S. M.: A single parameter representation of hygroscopic growth and cloud  
675 condensation nucleus activity, *Atmos. Chem. Phys.*, 7, 1961–1971, doi: 10.5194/acp-7-1961-2007, 2007.

676 Ren, J. Y., Zhang, F., Wang, Y. Y., Collins, D., Fan, X. X., Jin, X. A., Xu, W. Q., Sun, Y. L., Cribb, M., and  
677 Li, Z. Q.: Using different assumptions of aerosol mixing state and chemical composition to predict CCN  
678 concentrations based on field measurements in urban Beijing, *Atmos. Chem. Phys.*, 18, 6907–6921, doi:  
679 10.5194/acp-18-6907-2018, 2018.

680 [Rose, D., Nowak, A., Achtert, P., Wiedensohler, A., Hu, M., Shao, M., Zhang, Y., Andreae, M. O., and  
681 Pöschl, U.: Cloud condensation nuclei in polluted air and biomass burning smoke near the mega-city  
682 Guangzhou, China – Part 1: Size-resolved measurements and implications for the modeling of aerosol  
683 particle hygroscopicity and CCN activity, \*Atmos. Chem. Phys.\*, 10, 3365–3383,  
684 <https://doi.org/10.5194/acp-10-3365-2010>, 2010.](#)

685 Saarnio, K., Frey, A., Niemi, J. V., Timonen, H., Rönkkö T., Karjalainen, P., Vestenius, M., Teinilä K.,  
686 Pirjola, L., Niemelä V., Keskinen, J., Häyrinen, A., and Hillamo, R.: Chemical composition and size of  
687 particles in emissions of coal-fired power plant with flue gas desulphurization, *J. Aerosol Sci.*, 73, 14–26,  
688 2014.

689 [Schill, S. R., Collins, D. B., Lee, C., Morris, H. S., Novak, G. A., and Prather, K. A.: The impact of aerosol  
690 particle mixing state on the hygroscopicity of sea spray aerosol. \*ACS Central Science\*, 1\(3\), 132-141,  
691 2015](#)

带格式的: 图案: 清除 (白色)

692 Sjogren, S., Gysel, M., Weingartner, E., Baltensperger, U., Cubison, M. J., Coe, H., Zardini, A. A., Marcolli,  
693 C., Krieger, U. K., and Peter, T.: Hygroscopic growth and water uptake kinetics of two-phase aerosol  
694 particles consisting of ammonium sulfate, adipic and humic acid mixtures, *J. Aerosol Sci.*, 38, 157–171,  
695 doi: 10.1016/j.jaerosci.2006.11.005, 2007.

696 [Suda, S. R., Petters, M. D., Matsunaga, A., Sullivan, R. C., Ziemann, P. J., and Kreidenweis, S. M.:](#)  
697 [Hygroscopicity frequency distributions of secondary organic aerosols. \*J. Geophys. Res.\*, 117\(D4\), D04207,](#)  
698 [2012](#)

699 Svenningsson, B., Rissler, J., Swietlicki, E., Mircea, M., Bilde, M., Facchini, M. C., Decesari, S., Fuzzi, S.,  
700 Zhou, J., Mønster, J., and Rosenørn, T.: Hygroscopic growth and critical supersaturations for mixed  
701 aerosol particles of inorganic and organic compounds of atmospheric relevance, *Atmos. Chem. Phys.*, 6,  
702 1937–1952, doi: 10.5194/acp-6-1937-2006, 2006.

703 Sun, Y. L., Wang, Z. F., Du, W., Zhang, Q., Wang, Q. Q., Fu, P. Q., Pan, X. L., Li, J., Jayne, J., and  
704 Worsnop, D. R.: Long-term real-time measurements of aerosol particle composition in Beijing, China:  
705 Seasonal variations, meteorological effects, and source analysis, *Atmos. Chem. Phys.*, 15, 10149–10165,  
706 doi: 10.5194/acp-15-10149-2015, 2015.

707 Sun, Y., Du, W., Fu, P., Wang, Q., Li, J., Ge, X., Zhang, Q., Zhu, C., Ren, L., Xu, W., Zhao, J., Han, T.,  
708 Worsnop, D. R., and Wang, Z.: Primary and secondary aerosols in Beijing in winter: sources, variations  
709 and processes, *Atmos. Chem. Phys.*, 16, 8309–8329, doi: 10.5194/acp-16-8309-2016, 2016.

710 Swietlicki, E., Hansson, H. C., Hämeri, K., Svenningsson, B., Massling, A., McFiggans, G., McCurry, P.  
711 H., Petäjä, T., Tunved, P., Gysel, M., Topping, D., Weingartner, E., Baltensperger, U., Rissler, J.,  
712 Wiedensohler, A., and Kulmala, M.: Hygroscopic properties of submicrometer atmospheric aerosol  
713 particles measured with H-TDMA instruments in various environments - a review, *Tellus B*, 60, 432–469,  
714 doi: 10.1111/j.1600-0889.2008.00350.x, 2008.

715 Tan, H., Xu, H., Wan, Q., Li, F., Deng, X., Chan, P. W., Xia, D., and Yin, Y.: Design and application of an  
716 unattended multifunctional H-TDMA system, *J. Atmos. Ocean. Tech.*, 30, 1136–1148, doi:  
717 10.1175/JTECH-D-12-00129.1, 2013.

718 Turpin, B. J. and Lim, H. J.: Species contributions to PM<sub>2.5</sub> mass concentrations: Revisiting common  
719 assumptions for estimating organic mass, *Aerosol Sci. Tech.*, 35, 602–610, doi:  
720 10.1080/02786820152051454, 2001.

721 Wang, J., Cubison, M. J., Aiken, A. C., Jimenez, J. L., and Collins, D. R.: The importance of aerosol mixing  
722 state and size-resolved composition on CCN concentration and the variation of the importance with  
723 atmospheric aging of aerosols, *Atmos. Chem. Phys.*, 10, 7267–7283, doi:10.5194/acp-10-7267-2010,  
724 2010.

725 Wang, J., Zhang, Q., Chen, M.-D., Collier, S., Zhou, S., Ge, X., Xu, J., Shi, J., Xie, C., Hu, J., Ge, S., Sun,  
726 Y., and Coe, H.: First chemical characterization of refractory black carbon aerosols and associated  
727 coatings over the Tibetan Plateau (4730 m a.s.l), *Environ. Sci. Tech.*, 51, 14072,  
728 doi:10.1021/acs.est.7b03973, 2017.

729 Wang, J. F., Liu, D. T., Ge, X. L., Wu, Y. Z., Shen, F. Z., Chen, M. D., Zhao, J., Xie, C. H., Wang, Q. Q.,  
730 Xu, W. Q., Zhang, J., Hu, J. L., Allan, J., Joshi, R., Fu, P. Q., Coe, H., and Sun, Y. L.: Characterization of  
731 black carbon-containing fine 10 particles in Beijing during wintertime, *Atmos. Chem. Phys.*, 19, 447–458,  
732 doi: 10.5194/acp-19-447-2019, 2019.

733 Wang, Q., Zhao, J., Du, W., Ana, G., Wang, Z., Sun, L., Wang, Y., Zhang, F., Li, Z., Ye, X., and Sun, Y.:  
734 Characterization of submicron aerosols at a suburban site in central China, *Atmos. Environ.*, 131, 115–  
735 123, doi:10.1016/j.atmosenv.2016.01.054, 2016.

736 Wang, S. C. and Flagan, R. C.: Scanning Electrical Mobility Spectrometer, *Aerosol Sci. Tech.*, 13, 230–240,  
737 1990.

738 Wang, Y., Zhang, F., Li, Z., Tan, H., Xu, H., Ren, J., Zhao, J., Du, W., and Sun, Y.: Enhanced  
739 hydrophobicity and volatility of submicron aerosols under severe emission control conditions in Beijing,  
740 *Atmos. Chem. Phys.*, 17, 5239–5251, doi: 10.5194/acp-17-5239-2017, 2017.

741 Wang Y., Li Z., Zhang Y., Du W., Zhang F., Tan H., Xu H., Fan T., Jin X., Fan X., Dong Z., Wang Q. and  
742 Sun Y.: Characterization of aerosol hygroscopicity, mixing state, and CCN activity at a suburban site in  
743 the central North China Plain, *Atmos. Chem. Phys.*, 18, 11739–11752, doi: 10.5194/acp-18-11739-2018,  
744 2018a.

- 745 Wang, Y., Z. Wu, N. Ma, Y. Wu, L. Zeng, C. Zhao, and A. Wiedensohler: Statistical analysis and  
746 parameterization of the hygroscopic growth of the sub-micrometer urban background aerosol in Beijing,  
747 *Atmos. Environ.*, 175, 184-191, doi: 10.1016/j.atmosenv.2017.12.003, 2018b.
- 748 Wex, H., Petters, M. D., Carrico, C. M., Hallbauer, E., Massling, A., McMeeking, G. R., Poulain, L., Wu, Z.,  
749 Kreidenweis, S. M., and Stratmann, F.: Towards closing the gap between hygroscopic growth and  
750 activation for secondary organic aerosol: Part 1—Evidence from measurements, *Atmos. Chem. Phys.*, 9,  
751 3987–3997, doi: 10.5194/acp-9-3987-2009, 2009
- 752 Wu, Z., Hu, M., Lin, P., Liu, S., Wehner, B., and Wiedensohler, A.: Particle number size distribution in the  
753 urban atmosphere of Beijing, China, *Atmos. Environ.*, 42, 7967–7980, doi:  
754 10.1016/j.atmosenv.2008.06.022, 2008.
- 755 Wu, Z. J., Poulain, L., Henning, S., Dieckmann, K., Birmili, W., Merkel, M., van Pinxteren, D., Spindler, G.,  
756 Müller, K., Stratmann, F., Herrmann, H., and Wiedensohler, A.: Relating particle hygroscopicity and  
757 CCN activity to chemical composition during the HCCT-2010 field campaign, *Atmos. Chem. Phys.*, 13,  
758 7983–7996, doi: 10.5194/acp-13-7983-2013, 2013.
- 759 Wu, Z. J., Zheng, J., Shang, D. J., Du, Z. F., Wu, Y. S., Zeng, L. M., Wiedensohler, A., and Hu, M.: Particle  
760 hygroscopicity and its link to chemical composition in the urban atmosphere of Beijing, China, during  
761 summertime, *Atmos. Chem. Phys.*, 16, 1123–1138, doi: 10.5194/acp-16-1123-2016, 2016.
- 762 Xu, W. Q., Sun, Y. L., Chen, C., Du, W., Han, T. T., Wang, Q. Q., Fu, P. Q., Wang, Z. F., Zhao, X. J., Zhou,  
763 L. B., Ji, D. S., Wang, P. C., and Worsnop, D. R.: Aerosol composition, oxidation properties, and sources  
764 in Beijing: results from the 2014 Asia-Pacific Economic Cooperation summit study, *Atmos. Chem. Phys.*,  
765 15, 13681–13698, doi: 10.5194/acp-15-13681-2015, 2015.
- 766 Ye, X., Tang, C., Yin, Z., Chen, J., Ma, Z., Kong, L., Yang, X., Gao, W., and Geng, F.: Hygroscopic growth  
767 of urban aerosol particles during the 2009 Mirage-Shanghai Campaign, *Atmos. Environ.*, 64, 263–269,  
768 doi: 10.1016/j.atmosenv.2012.09.064, 2013.
- 769 Zardini, A. A., Sjogren, S., Marcolli, C., Krieger, U. K., Gysel, M., Weingartner, E., Baltensperger, U., and  
770 Peter, T.: A combined particle trap/HTDMA hygroscopicity study of mixed inorganic/organic aerosol  
771 particles, *Atmos. Chem. Phys.*, 8, 5589–5601, doi: 10.5194/acp-8-5589-2008, 2008

Zhang, F., Li, Y., Li, Z., Sun, L., Li, R., Zhao, C., Wang, P., Sun, Y., Liu, X., Li, J., Li, P., Ren, G., and Fan, T.: Aerosol hygroscopicity and cloud condensation nuclei activity during the AC3Exp campaign: Implications for cloud condensation nuclei parameterization, *Atmos. Chem. Phys.*, 14, 13423–13437, doi: 10.5194/acp-14-13423-2014, 2014.

Zhang, F., Li, Z., Li, Y., Sun, Y., Wang, Z., Li, P., Sun, L., Wang, P., Cribb, M., Zhao, C., Fan, T., Yang, X., and Wang, Q.: Impacts of organic aerosols and its oxidation level on CCN activity from measurement at a suburban site in China, *Atmos. Chem. Phys.*, 16, 5413–5425, doi: 10.5194/acp-16-5413-2016, 2016.

Zhang, F., Wang, Y., Peng, J., Ren, J., Zhang, R., Sun, Y., Collin, D., Yang, X., and Li, Z.: Uncertainty in predicting CCN activity of aged and primary aerosols, *J. Geophys. Res.-Atmos.*, 122, 11723–11736, doi: 10.1002/2017JD027058, 2017.

Zhang, R., Khalizov, A. F., Pagels, J., Zhang, D., Xue, H., and McMurry, P. H.: Variability in morphology, hygroscopicity, and optical properties of soot aerosols during atmospheric processing, *PNAS*, 105(30), 10291–10296, doi:10.1073/pnas.0804860105, 2008.

[Zhang, R., Wang, G., Guo, S., Zamora, M. and Wang, Y.: Formation of urban fine particulate matter. \*Chemical Reviews\*, 115\(10\), 3803-3855, 2015](#)

Zhang, Q., Stanier, C. O., Canagaratna, M. R., Jayne, J. T., Worsnop, D. R., Pandis, S. N., & Jimenez, J. L. : Insights into the chemistry of new particle formation and growth events in Pittsburgh based on aerosol mass spectrometry, [Environmental Science & Technology; Environ. Sci. Tech.](#), 38(18), 4797–4809, doi: 10.1021/es035417u, 2004.

[Zhang, Y., Zhang, Q., Cheng, Y., Su, H., Kecorius, S., Wang, Z., Wu, Z., Hu, M., Zhu, T., Wiedensohler, A., and He, K.: Measuring the morphology and density of internally mixed black carbon with SP2 and VTDMA: new insight into the absorption enhancement of black carbon in the atmosphere, \*Atmos. Meas. Tech.\*, 9, 1833-1843, 2016.](#)

Zhao, J., Du, W., Zhang, Y., Wang, Q., Chen, C., Xu, W., Han, T., Wang, Y., Fu, P., Wang, Z., Li, Z., and Sun, Y.: Insights into aerosol chemistry during the 2015 China Victory Day parade: results from simultaneous measurements at ground level and 260 m in Beijing, *Atmos. Chem. Phys.*, 17, 3215–3232, doi: 10.5194/acp-17-3215-2017, 2017.